universität wien

MASTERARBEIT / MASTER'S THESIS

Titel der Masterarbeit / Title of the Master's Thesis

„The Role of Activin A in Squamous Cell Carcinoma of the Lung"

verfasst von / submitted by

David Szabo, B.Sc.

angestrebter akademischer Grad / in partial fulfilment of the requirements for the degree of

Master of Science (MSc)

Wien, 2019 / Vienna 2019

Studienkennzahl lt. Studienblatt / degree programme code as it appears on the student record sheet:	UA 066 830
Studienrichtung lt. Studienblatt / degree programme as it appears on the student record sheet:	Molekulare Mikrobiologie, Mikrobielle Ökologie und Immunbiologie
Betreut von / Supervisor:	Univ. Prof. Dr. Walter Klepetko

Abstract

Lung cancer (LC) is the leading cause of cancer death worldwide accounting for 1.6 million deaths annually of which 30-50% are squamous cell carcinoma (SCC) cases with limited therapeutic options and poor prognosis. Therefore, there is a growing interest in biomarker-driven, non-invasive early diagnostic options. The role of Activin A has been investigated in various cancer types, including thoracic malignancies like lung adenocarcinoma (LADC) and malignant pleural mesothelioma (MPM) but not in SCC. According to our preliminary data analyzing SCC patients' blood samples showed significantly elevated ActA levels compared to healthy individuals. To establish the possible source of the elevated, TGF-β family cytokine, ActA we sought to determine the expression of ActA and activin receptors on the mRNA (q-RT-PCR) and protein (ELISA) level as well as the impact of ActA treatment on SCC cell lines using EZ4U assay kit. To this end our group received 10 SCC and 1 LADC cell line that have been cultivated in appropriate cell culture medium which involved regular examination under phase-contrast microscope to monitor their morphology. Medium was changed and the cells were passaged depending on the metabolic activity and growth rate of the particular cell line. When the cells were approximately 80% confluent, they were washed twice in phosphate buffered saline (PBS) and harvested in TRIzol reagent and RIPA lysis buffer for mRNA and protein isolation, respectively. The measured ActA levels via q-PCR showed positive correlation with the results obtained from ELISA assays. According to the aforementioned analyses the cell lines VL3, VL7, VL8, LUTCML-54 all secreted high amount of ActA on the mRNA as well as on protein levels. On the other hand, in cell lines SK-MES-01, VL1, VL5, VL9 were neither detectable ActA mRNA nor ActA protein which, in fact, further reinforces the concordance of the results. As it was mentioned before, the subunits of the ActA receptors has also been determined via q-PCR. The mRNA expression of the receptors' subunits assumes an inducible ActA signaling which was later validated by western blot where phosphor-Smad2/3 (P-Smad2/3) was detected upon human recombinant ActA treatment. The analysis of 43 SCC patients' blood revealed, that plasma ActA levels were significantly elevated in SCC patients in contrast to healthy people.

To choose a reliable cell line for future *in vivo* experiments, tumorigenicity assay was designed to evaluate the tumor forming capacity of the acquired non-small cell lung cancer (NSCLC) cell lines in immunodeficient xenograft mouse models via subcutaneous administration.

Zusammenfassung

Lungenkrebs (LC) ist die weltweit häufigste Todesursache bei Krebs mit 1,6 Millionen Todesfällen pro Jahr, von denen 30-50% Plattenepithelkarzinomen (PEC) mit eingeschränkten therapeutischen Möglichkeiten und schlechter Prognose sind. Daher besteht ein wachsendes Interesse an biomarker-getriebenen, nicht-invasiven Frühdiagnosemöglichkeiten. Die Rolle von Activin A (ActA) wurde bei verschiedenen Krebsarten untersucht, einschließlich maligner Erkrankungen des Brustraums wie das Adenokarcinom der Lunge (LADC) und malignem Pleuramesotheliom (MPM), jedoch nicht bei PEC. Nach unseren vorläufigen Daten, die die Blutproben von PEC-Patienten analysiert haben, zeigten sich im Vergleich zu gesunden Personen signifikant erhöhte ActA-Werte. Um die mögliche Quelle des erhöhten Zytokins der TGF-β-Familie, ActA, zu bestimmen, haben wir versucht, die Expression von ActA- und Activin-Rezeptoren auf der Ebene von mRNA (q-RT-PCR) und Protein (ELISA) zu bestimmen. Auch wurde die Auswirkung der ActA-Behandlung auf SCC-Zelllinien unter Verwendung des EZ4U-Assay-Kits analysiert. Zu diesem Zweck erhielt unsere Gruppe 10 PEC- und 1 LADC-Zelllinien, die in einem geeigneten Zellkulturmedium kultiviert wurden, das eine regelmäßige Untersuchung unter einem Phasenkontrastmikroskop zur Überwachung ihrer Morphologie umfasste. Das Medium wurde gewechselt und die Zellen wurden in Abhängigkeit von der Stoffwechselaktivität und der Wachstumsrate der jeweiligen Zelllinie passagiert. Wenn die Zellen zu ungefähr 80% konfluent waren, wurden sie zweimal in phosphatgepufferter Salzlösung (PBS) gewaschen und in TRIzol-Reagenz und RIPA-Lysepuffer für die mRNA- bzw. Proteinisolierung geerntet. Die mittels q-PCR gemessenen ActA-Spiegel zeigten eine positive Korrelation mit den Ergebnissen des ELISA-Tests. Gemäß den zuvor genannten Analysen sezernierten die Zelllinien VL3, VL7, VL8, LUTCML-54 alle eine hohe Menge an ActA auf der mRNA sowie auf die Proteinebene. Andererseits war in den Zelllinien SK-MES-01, VL1, VL5, VL9 weder ActA-mRNA noch ActA-Protein nachweisbar, was in der Tat die Übereinstimmung der Ergebnisse weiter verstärkt. Wie bereits erwähnt, wurden die Untereinheiten der ActA-Rezeptoren auch über q-PCR bestimmt. Die mRNA-Expression der Rezeptor-Untereinheiten setzt eine induzierbare ActA-Signalisierung voraus, die später durch Western Blot validiert wurde, wobei Phosphor-Smad2/3 (P-Smad2/3) nach rekombinanten ActA-

Behandlung nachgewiesen wurde. Die Analyse von 43 PEC-Patientenblut ergab, dass die Plasma-ActA-Spiegel bei PEC-Patienten im Gegensatz zu gesunden Menschen signifikant erhöht waren.

Um eine zuverlässige Zelllinie für zukünftige In-vivo-Experimente auszuwählen, wurde ein Tumorigenitätstest entwickelt. Dabei wurde die Tumorbildungskapazität der erworbenen nicht-kleinzelligen Lungenkrebs (NSCLC) -Zelllinien in immundefizienten Xenotransplantat-Mausmodellen durch subkutane Verabreichung bewertet.

Table of Contents

1 Introduction

1.1 Epidemiology of Lung Cancer

With more than 3.7 million new cases and 1.9 million deaths annually, cancer represents the second most frequent cause of death and morbidity in Europe. (WHO #1) Lung cancer is the biggest killer worldwide, responsible for approximately 1.6 million deaths each year. [1]. The biggest culprit no doubt is tobacco smoking but air pollution and well known human carcinogens e.g. crystalline silica and chrysotile asbestos also increase lung cancer risk.[2] Despite recent advances in radiotherapy, chemotherapy video-assisted thoracic surgery (VATS), the five year survival rate of patients remain around 60%. [3] [4] Unfortunately, screening for lung cancer is at the time not recommended by any major medical organization, although, it has been shown that computer tomography (CT) scans readily detect 10-15 mm sized lung cancers whereas chest X-rays missed 70-80% of cancers detected by CTs. Therefore, screening patients with high risk developing lung cancer might confer to early detection thus better prognosis through early intervention.

1.2 Squamous cell lung cancer

Lung cancers are divided into two major groups: non-small cell (NSCLC) and small-cell lung cancer (SCLC), where NSCLC represents 80-85% of all cases. NSCLC further classified into three subtypes where squamous-cell carcinoma (SCC) and adenocarcinoma account for the majority of NSCLC cases. [5]. SCC is the second largest histological subtype responsible for ~30% of all NSCLC cases [6]. Although, tobacco smoking is strongly associated with all the major histological subtypes of NSCLC, SCC patients more often have a history of heavy tobacco abuse with one study suggesting 91% of SCC was attributed to cigarette smoking [7].

1.2.1 Risk factors and genetic mutations related to Squamous cell carcinoma

Tobacco smoking is also a predominant risk factor for chronic obstructive pulmonary disease (COPD). COPD is characterized by an excessive inflammatory and oxidative stress response, hence the progressive airflow obstruction which greatly favors to malignant transformation: carcinogenesis. I have been involved in a cohort study, where I was assigned to search for SCC patients' clinical and pathological data in the National Koranyi Institute of TB and Pulmonology (Budapest, Hungary) databank. In my research I reported that 65% of the SCC patients were also diagnosed with COPD and moreover, all of those patients were almost exclusively active smokers and in a small percentage ex-smokers. Papi et. al. confirmed our observations, they found that approximately 70% of the SCC patients indeed suffered from COPD [8]. Inherited genetic susceptibility as well as acquired genetic alterations in oncogenic pathways confer greatly to lung cancer tumorigenesis. Relative frequency comparison of differential driver mutations in adenocarcinoma, SCC and COPD patients summarized in **Table 1**. [9] [10] [11] Lung SCCs are characterized by high overall mutation rate which is rather typical in case of smokers. Almost all lung SCC contain somatic mutation of TP53 and there are also recurrent alterations in the following oncogenic pathways: CDKN2A/RB1, PI3K/AKT, FGFR/KRAS pathways suggesting a malfunctioning cell cycle control, response to apoptotic signaling and growth stimulus. [10] [12] Unfortunately, ALK fusion and activating mutations in EGFR are a rare event in lung SCC, thus the targeted therapies widely and successfully used in adenocarcinoma patients are generally ineffective against squamous cell carcinoma.

Table 1| Genetic aberration reported in Lung associated disease [9] [10] [11]

Genetic alterations	Adenocarcinoma	Squamous cell carcinoma	COPD
EGF receptor mutations	5–15% frequency	infrequent	EGF receptor amplification occurs
ELM4/ALK translocations	5–15% frequency	infrequent	Not detected
KRAS mutations	>15% frequency	infrequent	Not detected
FGFR family amplification/overexpression	infrequent	20% frequency in FGFR1 amplification	Overexpression of FGF1/2 and FGFR1 detected
PI3KCA amplification	infrequent	>30% frequency	Increased PI3K pathway activation
Loss of PTEN status	infrequent	Mutations and methylation detected (10-40% frequency)	PTEN pathway down-regulated
TP53 mutations	>40% frequency	90% frequency of inactivating mutation	-
Inactivation of CDKN2A (encodes for p16INK4A and p14ARF cell cycle regulators)	>40% frequency	70% frequency	-

1.2.2 Diagnosis and treatment

Despite the recent progress in NSCLC treatment, the patients' 5-year survival chances remain rather modest. Generally, the treatment of lung cancer is based on the stage of disease, performance status, histological type (ie. NSCLC, SCLC) and more recently, tumor related genetic aberrations are also taken into account. [13] However, most patients will likely not benefit from the targeted therapies (gefitinib, bevacizumab) successfully used in adenocarcinoma patients, thus novel effective SCC specific therapy regimens have to evolve to improve overall survival for the patients suffering from squamous cell lung cancer. [14] Currently, the best treatment option, if feasible, is surgical resection. Video-assisted surgery (VATS) has become widely adopted which made the surgical approach even more favorable. VATS has been reported to shorten hospital stay, accelerate recovery, decrease postoperative complications whereas overall survival and

recurrence rate did not show significant difference. [15] Nevertheless, patients with potentially resectable tumor must qualify as fit, regarding their age, pulmonary function and cardiovascular health. [16] Unfortunately, many patients fail to meet the criteria mostly because of their advanced stages, lymph node involvement and detected invasion of the chest wall. [17] [18] Those with advanced, inoperable SCC platinum-based chemotherapy and concurrent radiotherapy is the first-line option. In order to minimalize acquired resistance, combination therapies with a second therapeutic agent is highly recommended. Examples for combination therapies listed in **Table 2**. Platinum based agents (cisplatin, carboplatin) covalently bind to DNA and induce apoptosis through the activation of DNA-damage checkpoints. This, in fact, is the Achilles' heel of the cytostatic drugs due to the reported high mutation rate of TP53 tumor suppressor in SCC which is one of the most important factor in cell cycle arrest and programmed cell death promotion. [19] Taxane, a DNA demaging agent hinders replication (e.g. paclitaxel or docetaxel). Gemcitabin, on the other hand, is an example for DNA incorporating agent which when in incorporated eludes the cells' DNA repair system. The faulty nucleotide considered irreparable that leads to abrogation of further DNA synthesis and thus, cell death. Topoisomerase II inhibitors such as etoposide and doxorubicin generate DNA lesions resulting in DNA strand breaks. [20] [21] Personalized treatment include monoclonal antibodies (mAb) as checkpoint inhibitors (e.g. CTLA-4, PD-1, PDL-1) and receptor tyrosine kinase inhibitors (e.g. vascular endothelial growth factor - ramucirumab). The unambiguous advantage of mAbs is that they are less likely to harm healthy cells, although side effects do appear in form of autoimmunity and overwhelming inflammation. [22] Whereas receptor tyrosine kinase inhibitors block the downstream activation of oncogenic pathways, immunotherapy focuses on the stimulation of the immune system by restoring antitumor immunity. I previously explained the recent improvements in NSCLC disease management especially in lung adenocarcinoma. In contrast, the progress in SCC has been modest due to the lack of overlapping genetic alterations with adenocarcinoma. Therefore, there has been a growing interest to acquire better understanding of the genetic alterations that drive SCC as well as to identify potential therapeutic targets. [23] The phosphatidylinositol 3-kinase (PIK3CA) is one of the most researched pathway associated with SCC. Buparlisib (BKM120) a PI3K inhibitor is currently in phase II trials, showing great

potential as a future target. The fibroblast growth factor receptor 1 (FGFR1) is also reported to be overexpressed in SCC. Upon positive *in vitro* studies brivanib (BMS-582664), an FGFR inhibitor, is now in early phase clinical trials. [24] Number of randomized clinical trials have been enrolled and the results are eagerly awaited. With these studies it is expected to maximize therapeutic benefits while attenuating toxicity of the drugs.

Table 2| Review of current and potential future therapies for advanced SCC *(adjusted by the author) [25] [26] [27]*

Cytotoxic chemotherapy	Docetaxel Carboplatin Cisplatin
Combination therapies	Cisplatin + Etoposide Carboplatin + Gemcitabine Atezolizumab + Carboplatin Ramucirumab + Docetacel
Anti-angiogenesis therapy	Ramucirumab
Immunotherapeutic targets	CTLA-4: ipilumab, tremelimumab PD-1: nivolumab, pembrolizumab PDL-1: BMS-936559, MPDL3280A, MEDI4736, atezolizumab
Future targets	PI3K-AKT pathway FGFR pathway IGF pathway

1.2.3 Potential diagnostic and prognostic biomarkers

There are no useful biomarkers for early detection of progressive SCC, therefore there is an urgent need to identify non-invasive biomarkers that have the potential to revolutionize the future health care including therapeutic decision making and improved prognostic value. Despite being one of the deadliest disease there are only few blood based biomarkers currently investigated in SCC: cancer antigen 125 (CA 125), carcinoembryonic antigen (CEA)[28], serum amyloid A (SEA) [29], heptaglobin-alpha 2 (HAP2) [30], apolipoprotein A1 (ApoA1) [31], laminin C2 (lamC2) [32], plasma fibrinogen [33], kallikreins (KLKs)[34]. Recently, the scientific community has begun to apply liquid biopsies, where liquid biomarkers can be isolated from various body fluids e.g. blood, saliva, urine, ascites, pleural effusion etc. Circulating tumor-derived markers such as circulating tumor cells (CTCs), cell-free nucleic acids (cfDNA, miRNA, lncRNA) and exosomes might be useful tools for diagnostic purposes [35] [36] There is a great potential in the aforementioned biomarkers, nevertheless the limitations of these techniques is still yet to overcome in the future.

1.3 Activin A: a versatile cytokine of the the TGF-β family

1.3.1 History, nomenclature and structure

Activins, multifunctional cytokines, are members of the transforming growth factor beta (TGF-β) family of growth and differentiation factors. [37] The activins were originally recognized in the 1980s as regulators of follicle-stimulating hormone (FSH) secretion from pituitary cells and were named “activins” because of their roles contrary to those of inhibins in this context. [38] [39] Since their discovery they have been associated with wide variety of biological processes starting from early stages of embryogenesis to exceptional functions in readily differentiated cells and tissues. More specifically, they are involved in inflammatory responses [40], stem cell biology [41], wound repair [42], regulation of female and male reproduction [43]. Reportedly, activins were expressed by $CD4^+$ $CD25^-$ T cells and B lymphocytes [44], M2 (alternative) macrophages [45], dendritic cells [46] and mast cells [47]. Activins consist of two ß subunits whereas inhibins appearing as αß

heterodimers. To date, four ß (ßA, ßB, ßC and ßE) and one α monomers have been reported in mammals. The ßA, ßB transcripts are present in most tissue type whereas ßC and ßE expression is mostly restricted to the liver. The internal dimerization of two ßA subunits called ActA [48].

1.3.2 Activin A receptors, signaling and regulation

ActA has two type I receptors (ALK-4 and ALK-7) together with two type II receptors (ActRIIa, ActRIIb) as illustrated in **Figure 1**. Inhibins, on the other hand, use a type II receptor and a type III TGF-β receptor (betaglycan). [48]

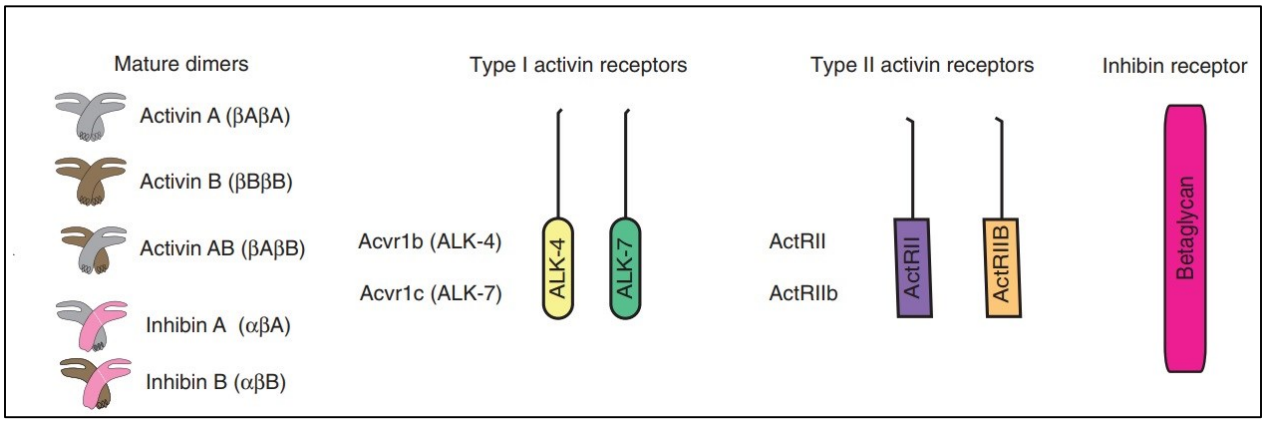

Figure 1| Ligands and receptors of activins and inhibins [43]

Activins are secreted from the cell while still bound to its protecting pro-domain. Binding to the type II receptor leads to the release of the associated pro-domains and subsequent dimerization as well as activation of the type II receptors' serine-threonine kinase activity. [49]. The resulted tetramer recruits two type I receptors, ALK-4 or ALK-7, and phosphorylates them. The assembled hexameric activin-receptor complex then triggers the phosphorylation of the regulatory Smad2 and Smad3 which in turn binds to Smad4. Upon nuclear translocation of the Smad complex, it acts as a transcriptional regulator together with other co-factors. [43]

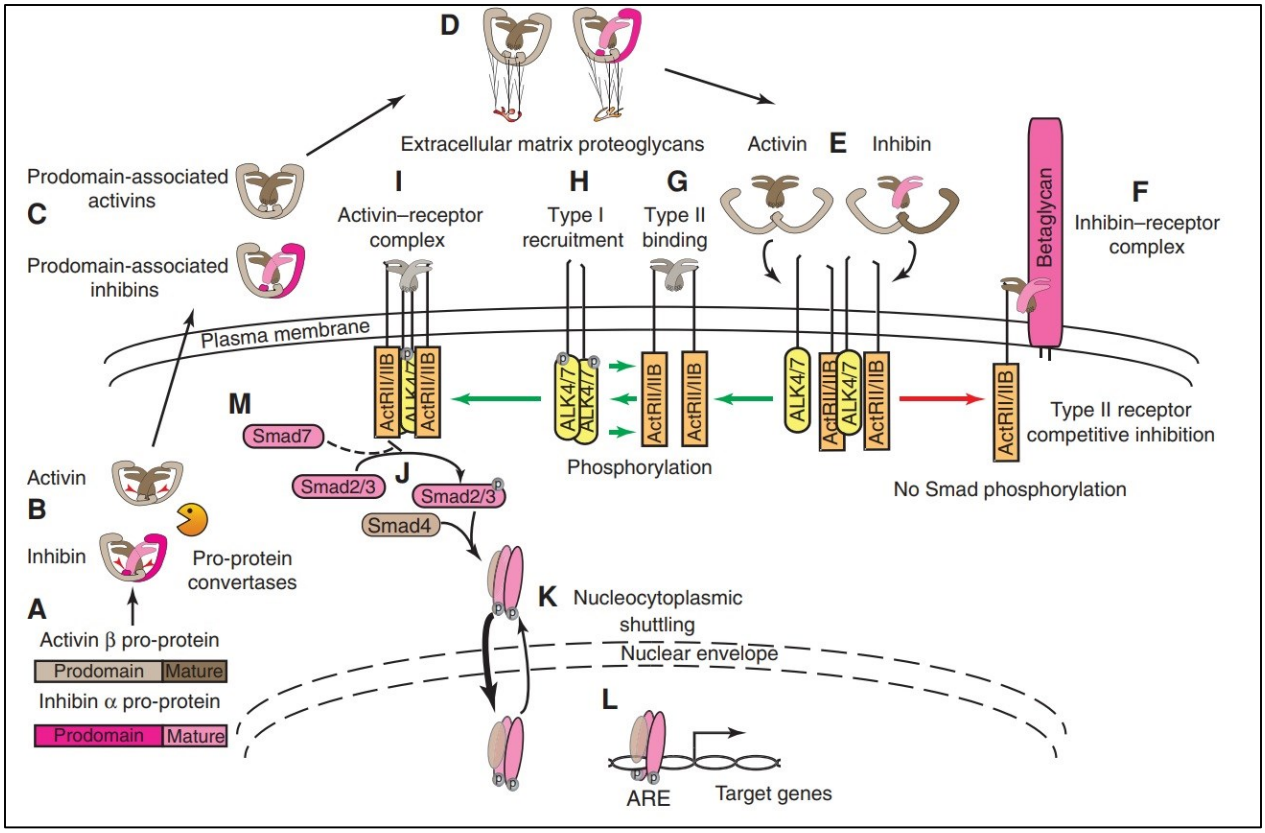

Figure 2| Activins' secretion and canonical signaling pathway [43]

Next to the aforementioned Smad-mediated signaling activins mediate various signaling pathways which does not require Smad phosphorylation. These include the MAP kinase pathway(MAPK), p38/JNK pathway as well as the PI3K/Akt pathway [50]. Inhibins are the best characterized regulator of activins, however the the ActA cascade can be regulated on various levels. Follistatin (FST) as a circulating (follistatin 315) and membrane bound (follistatin 288) form binds irreversibly to ActA covering its receptor binding domain. Other TGF-β family member can compete with activins for type II receptor binding, like inhibin uses the type II receptor forming a complex of inhibin-AcvRII-betaglycan, thereby antagonizing ActA signaling. Bone morphogenetic protein (BMP) and activin membrane-bound inhibitor (BAMBI) is structurally related to type I receptors but cannot phosphorylate Smads because the lack of kinase domain. In the cytoplasm Inhibitory Smad-7 interferes with Smad2/3 phosphorylation by binding to type I receptors and promotes its proteosomal degradation via Smurf2, an E3 ubiquitin ligase [51].

1.3.3 Activin A in cancer

As previously described, ActA is critically involved in cellular differentiation and maintenance of homeostatic state in multiple cell and tissue types. Consequently, malfunctioning ActA signaling has been reported in wide range of malignancies including breast [52] [53], lung [54], colon [55], prostate [56], ovary [57], liver [58], esophagus [59] as well as in melanoma [60]. Nevertheless, dysregulated ActA expression appears in both as protective and tumor promoting roles. These conflicting observation might be explained by the fact that in several non-transformed cell types, ActA induces growth arrest and apoptosis. Tumor cells, however, become resistant to activin-mediated growth inhibition and in turn, they often react with increased proliferation and aggressiveness [61]. Tumor cells are able to overcome growth limiting activin signals by for instance, overexpressing the activin antagonist FST that has been observed in hepatocellular and mammary carcinoma, respectively [53] [58] Another example is when colorectal cancer and pancreatic carcinoma cells acquire inactivating mutations in activin receptors. In these tumor types loss of Smad 4 has also been reported which would provide the nuclear translocation signal for the readily phosphorylated Smad2/3 complex [55]. In a recent study, it was demonstrated that Nuclear-factor-kappa B (NFκB) dependent overexpression of ActA in both LADC and SCC led to elevated epithelia-mesenchymal transition (EMT), promoting cancer cell invasion and metastasis. ActA can concomitantly support tumorigenesis by inducing the expression of vesicular endothelia growth factor (VEGF) and matrix metalloproteinases (MMP) which favors angiogenesis i.e. the synthesis of new blood vessels.

1.4 Previous work by our group on ActA in cancer, focusing on lung cancer

Previous studies by the Institute of Cancer Research of the Medical University of Vienna have demonstrated the tumor promoting role in malignant pleural mesothelioma (MPM) as well as in LADC. They found that both MPM and LADC patients had higher circulating ActA levels compared to healthy controls that also correlated with disease stage and worse overall survival(OS) [62] [63].

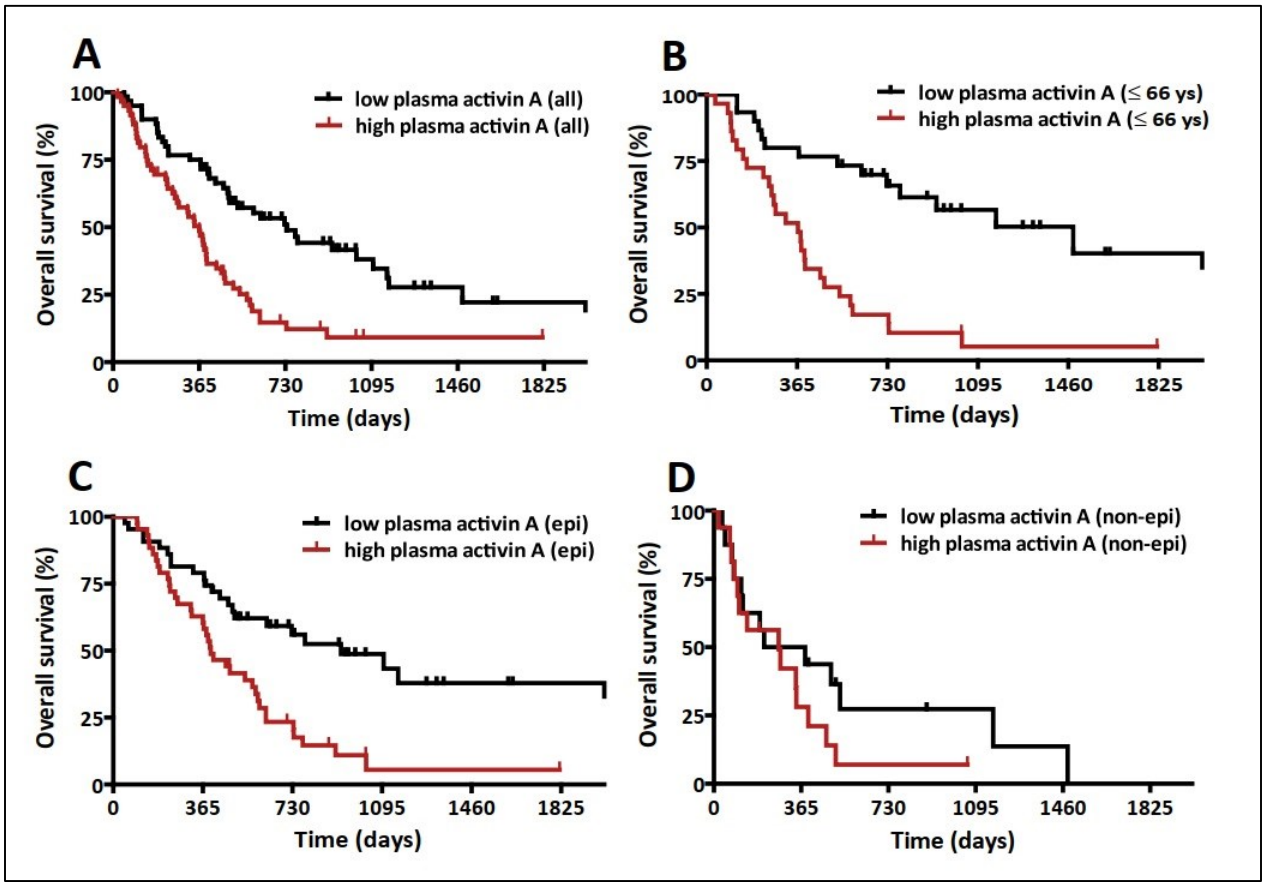

Figure 3| The prognostic value of circulating plasma ActA in various groups of MPM patients [63]

A, Kaplan-Meier survival analysis of all MPM patients (n= 119) **B,** ActA's prognostic power described only in patients younger than 66 years of age. **C,** High plasma levels of ActA in epithelioid MPM patients resulted in significant decrease in OS (n= 86) **D,** Interestingly, plasma levels of ActA had no impact on the OS in patients with non-epithelioid MPM (n= 32)

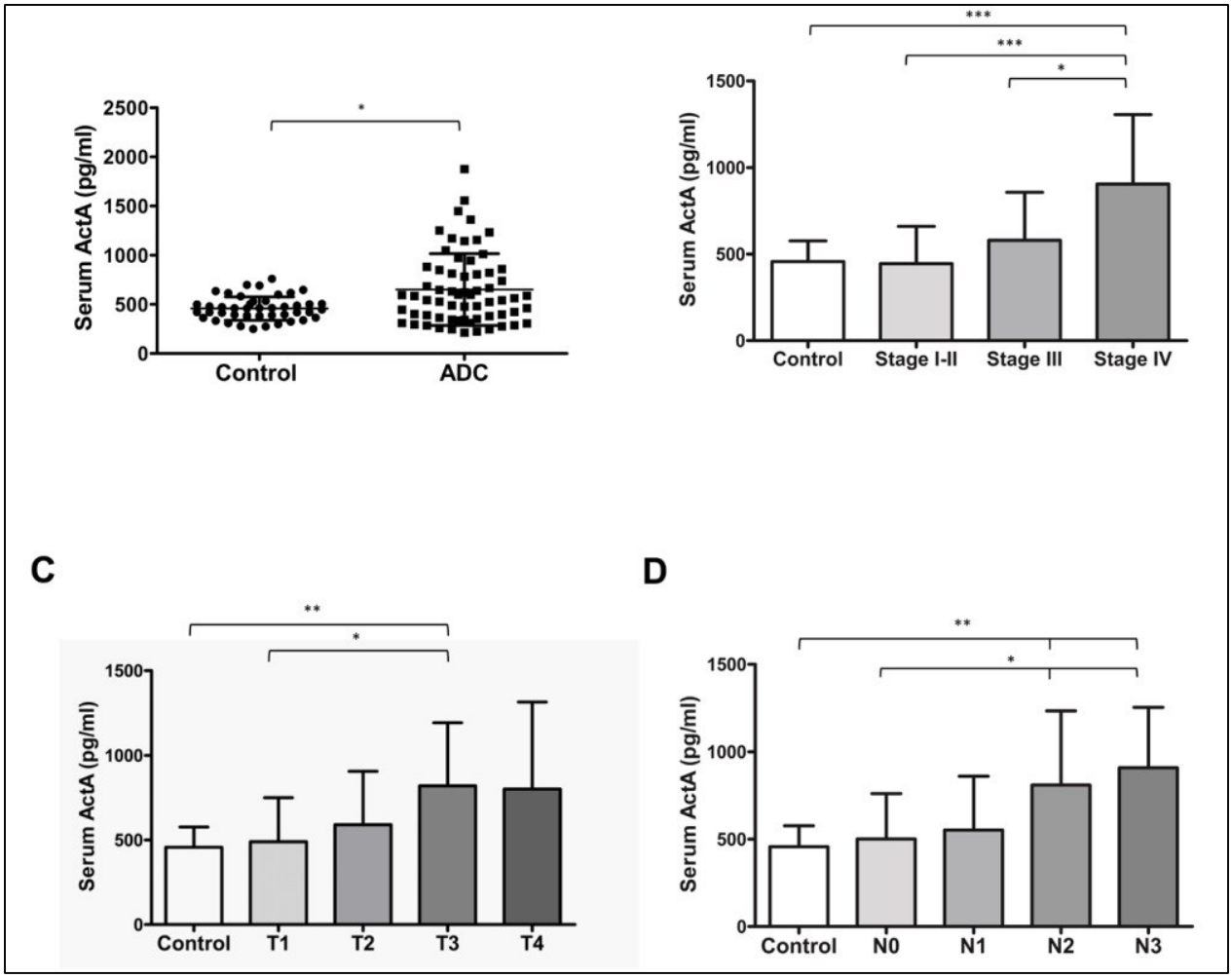

Figure 4| Stage dependently elevated serum ActA levels in LADC enhance tumor progression [62]

A. Plasma ActA concentration increased in LADC patients compared to healthy individuals **B., C., D.** T and N status – and stage – dependent elevation of serum ActA in LADC. T: refers to the original size of the primary tumor; N: regional lymph node involvement

Compared to other thoracic malignancies there is no available data regarding ActA expression and function in SCC. Our preliminary ELISA result, however, showed significantly elevated ActA levels in SCC patients compared to healthy controls. (**Figure 5**.) Moreover, high plasma ActA levels were correlated with more advanced stages and worse overall survival. (**Figure 8**; **Figure 9**.)

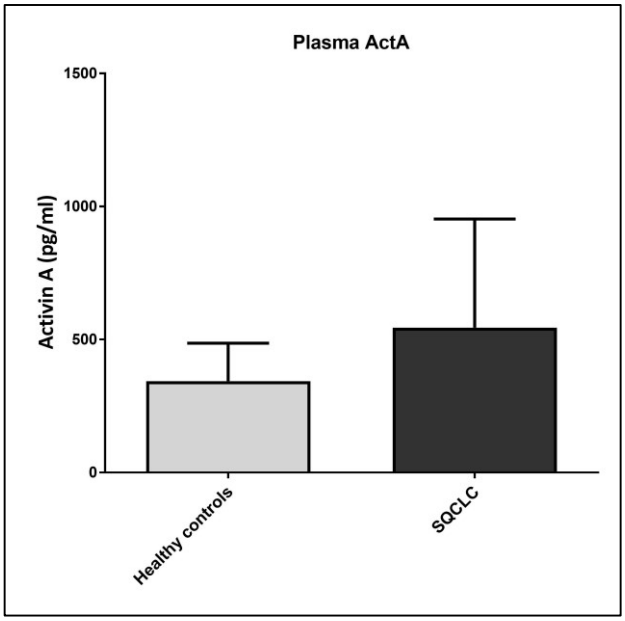

Figure 5| Preliminary results on ActA in squamous cell lung cancer patients. Significantly elevated ActA levels in SCC patients compared to healthy controls (n=37) *Contribution from Dr.Med.Thomas Klikovits, Medical University of Vienna*

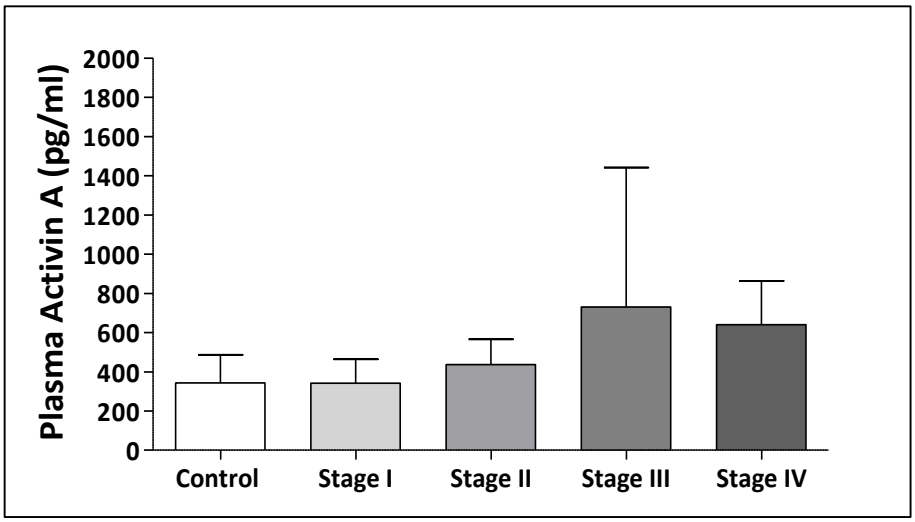

Figure 6| Preliminary results demonstrate a stage-dependent increase of circulating ActA in SCC patients. *Contribution from Dr.Med.Thomas Klikovits, Medical University of Vienna*

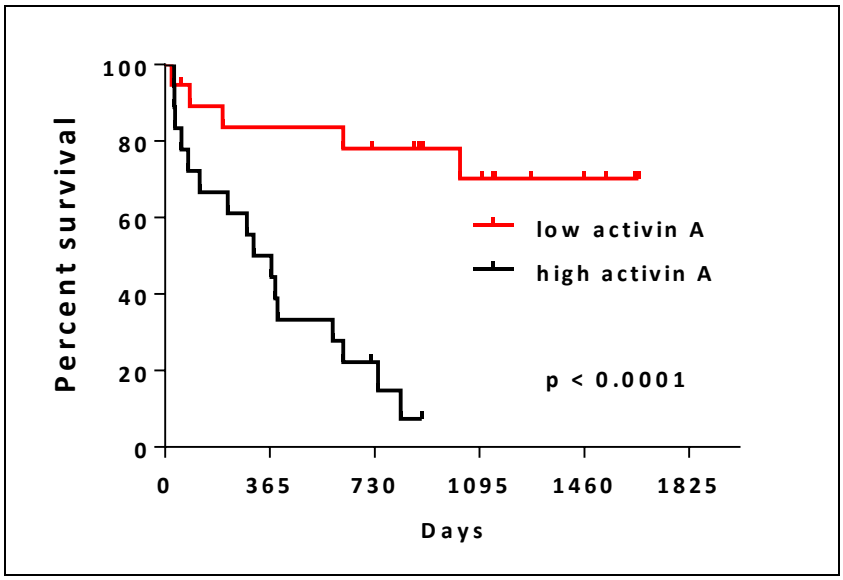

Figure 7| Preliminary result reinforce the prognostic value of ActA in SCC Kaplan-Meier survival analysis of SCC patients (n=37) Strong correlation between high ActA expression and worse OS *)*
Contribution from Dr.Med.Thomas Klikovits, Medical University of Vienna

2 Aims of the thesis

Based on the above depicted data and the available results on the function of ActA in various [16] tumor types, the aim of the thesis is to perform and to prepare for an in-depth investigation on the role of ActA in SCC.

Consequently, I will investigate:

1. The level of ActA in the plasma of an expanded cohort of SCC patients (ELISA)

2. The expression of ActA (INHBA gene) and activin receptors via RT-qPCR (Acvr1b, ActRIIa, ActRIIb)

3. The amount of intracellular and secreted ActA in NSCLC cell lines (ELISA)

4. The impact of recombinant activin treatment on *in vitro* proliferation (cell viability assay), and the induction of downstream signaling (Smad2/3 phosphorylation) via Western Blot

5. The ability of NSCLC cell lines to develop viable tumors in mice (tumorigenicity assay)

3 Materials and methods

3.1 Non-small cell lung cancer cell lines

Table 3|NSCLC patient and cell line characteristics*[64]*

Cell line	Patient			Cell line		
	Age (years)/sex	Site	Stage	Type[1]	Growth[2]	Medium
VL-1 (E14)[3]	54/m	lung	IIIa	Adenocarcinoma	26.9	DMEM
VL-3 (JH-WE)[3]	55/m	lung	I	Squamous	32.8	RPMI
VL-5 (MCKW)[3]	52/m	Lymph node	IIIa	Squamous	29.7	RPMI
VL-7 (MS-PG)[3]	62/m	Lymph node	IV	Squamous	39.3	RPMI
VL-8 (MB-SJ)[3]	68/m	Lymph node	IV	Squamous	31.7	RPMI
VL-9 (ZY-GF)[3]	64/m	lung	II	Squamous	30.6	RPMI
VL-10 (AH-WG)[3]	60/m	lung	II	Squamous	32.8	RPMI
SK-MES-01[4]	65/m	metastatic site pleural effusion	-	Squamous	-	RPMI
LUTCML-54[5]				Squamous	-	RPMI
SW900[4]	53/m	lung	IV	Squamous	-	RPMI

[1] Main histology of the primary tumor. – [2] Minimal doubling time in hr. – [3] established from surgical specimen at Medical University of Vienna Institute of Cancer Research; Walter Berger lab. – [4] obtained from University of Colorado (Denver, USA). – [5] DKFZ (Heidelberg, Germany).

Table 4|Mice squamous cell lung cancer cell characteristics*[65]*

Cell line	Cell line			
	Strain	**Site**	**Type**	**Medium**
KLN 205	DBA/2	lung	squamous	RPMI

3.2 Cell culture

All cell lines except VL-1 were grown in Sigma's RPMI-1640 medium in Cytoperm™ 2 CO_2 Gassed Incubator (Thermo Scientific, USA) at 37°C and 5% CO_2 supplemented with 10% bovine serum albumin (BSA) (Serva; Heidlberg, Germany) and 1% Penicillin-Streptomycin (Sigma-Aldrich, USA). The cell line VL-1 was cultivated in Dulbecco's modified Eagle medium (DMEM) (Sigma-Aldrich, USA) supplemented and stored as the RPMI-1640 medium. Splitting of adherent cells was performed with trypsin-EDTA solution (Sigma-Aldrich, USA). 10% DMSO (Sigma-Aldrich, USA) was diluted in appropriate medium for cell freezing. When mixed with DMSO, cell suspensions were transferred to cryo tubes and placed in CoolCell® Cell Freezing Container (BioCision, USA). The containers were stored at -80°C for 24 hours before transferred to liquid nitrogen.

3.3 RNA extraction, reverse transcription and Real Time quantitative-Polymerase Chain Reaction

RNA extraction was carried out via an RNeasy Mini kit (Qiugen, Netherlands). The manufacturer's protocol was followed with minor modifications during the procedure. In summary, when the cells were approximately 80% confluent, they were washed twice in pre-warmed phosphate buffered saline (PBS) and harvested in TRIzol reagent for mRNA isolation. Lysed cells were resuspended, aliquoted and stored at -80°C in RNase-free 1,5 mL Eppendorf tubes. After thawing the lysed cells, they were incubated for 5 minutes at room temperature. 200 µL chloroform was

added to each samples and were shaken for 15-20 seconds which was followed by a centrifugation (Beckman Coulter™ Microfuge® 22R) step at 15000g for 15 minutes. The upper layer containing the RNA of interest were transferred into a new RNase-free 1,5 Eppendorf tube while the middle layer was kept intact. 500 µL of isopropanol was added and gently mixed in the tube. The samples were incubated for 20 minutes on ice and then centrifuged at 4°C and 15000g for 15 minutes. The supernatant was removed and 1 mL 96% Ethanol was pipetted onto the pellet. The sample was centrifuged again using the same setting as previously. Finally, the supernatant was disposed and the isolated RNA was left out under the sterile hood to dry at RT for 30 min. The pellet was eluted with 20-50 µL nuclease-free water (depending on the size of the RNA pellet). The concentration and purity of the isolated RNA was measured via NanoDrop 8000 (Thermo Scienfitic, USA).

The mRNA template has to be reverse transcribed to cDNA for the RT-qPCR. The Reverse transcription (RT) master mix (High capacity cDNA Reverse Transcription Kit; Thermo Fischer, USA) was set up according to **Table 5**. The RT was performed with the Biometra T_{3000} Thermo Cycler according to the setup represented in **Table 6**. The RT-qPCR reaction was performed with a SYBR Green-containing master mix (GoTaq qPCR Master Mix; Promega, USA) as described in **Table 7**. 1 µL cDNA template was added to each well yielding the total volume of 11 µL. The resulted gene expression levels were normalized to Glyceraldehyde 3-phosphate dehydrogenase (GAPDH) house-keeping gene.

Table 5| Pipetting scheme for cDNA synthesis

Components	Volumes
10x RT Buffer	2 µL
25x dNTP Mix	0,8 µL
Multiscribe™ Reverse Transcriptase 50 U/µL	1 µL
10x Random Primer	2 µL
RNase Inhibitor	1 µL
Nuclease Free Water (NFW)	3,2 µL
RNA template	1 µg
Complete to final volume of 20 µL with NFW	

Table 6| Protocol on Thermocycler, Reverse transcription setup

cDNA synthesis step	Temperature	Time
Primer annealing	25 °C	10 min
DNA polymerization	37 °C	120 min
Enzyme inactivation	85 °C	5 min
Keep cool function	4 °C	24 h

Table 7| Pipetting scheme for RT-q-PCR preparation

Components	Volumes
TaqMan™ Gene Expression Master Mix	5 µL
TaqMan™ Assay (Primers)	0,5 µL
Nuclease Free Water	4,5 µL
cDNA sample	1 µL
Total	11 µL

Table 8| RT-q-PCR conditions for amplifications of our genes of interest

Cycles	PCR Step	Temperature	Time
1	Enzyme activation	50 °C	2 min
1	Initial Denaturation	95 °C	10 min
40	Denaturation	95 °C	15 sec
	Annealing	60 °C	1 min

Table 9| Primer DNA sequences of housekeeping and target genes

Gene		Primer sequence
INHBA	Forward	5' -CCCCTTTGCCAACCTCAAA- 3'
	Reverse	5' -CATGGACATGGGTCTCAGCTT- 3'
GAPDH	Forward	5' - GACAGTCAGCCGCATCTTCT- 3'
	Reverse	5' - TTAAAAGCAGCCCTGGTGAC- 3'
ACVR1B	Forward	5' -TCCTCCTTCTTCCCCCTTGTTG- 3'
	Reverse	5' - TGCTCCATCCCATCCAGATTG- 3'
ACVR2A	Forward	5- TGGCTCCAGAGGTATTA-3
	Reverse	5- CGCAACCATCATAGACT-3
ACVR2B	Forward	5- CTCATCACGGCCTTCCAT-3
	Reverse	5- AGCGAGCCTCTGCATCAT-3

3.4 Cell viability assay

The NSCLC cell lines were seeded to a 96-well plate as following:

Table 10| Seeded cell density to 96-well plate for cell viability assay

NSCLC cell line	Number of cells/well
VL-1	3000
VL-3	5000
VL-5	5000
VL-7	10000
VL-8	5000
VL-9	10000
VL-10	7500
LUTCML-54	5000
SK-MES-01	3000
KLN-205	2000

Activin A has been linked to either apoptosis induction or stimulation of tumor growth depending on the actual cell type. Therefore, the response of NSCLC cells to human recombinant (hr) ActA has been evaluated. Cells were seeded to 96-well plates as outlined in **Figure 8**. The next day, medium was replaced with fresh medium containing 20 ng/ml hr ActA or mock. After 72 hours of incubation in the cell culture incubator cell viability was measured with the EZ4U kit (Biomedica, Vienna, Austria) following the manufacturer's instructions. Readout for absorption of the red formazan, generated by the cells' mitochondria was performed at 450 nm and at 620 nm for wavelength correction.

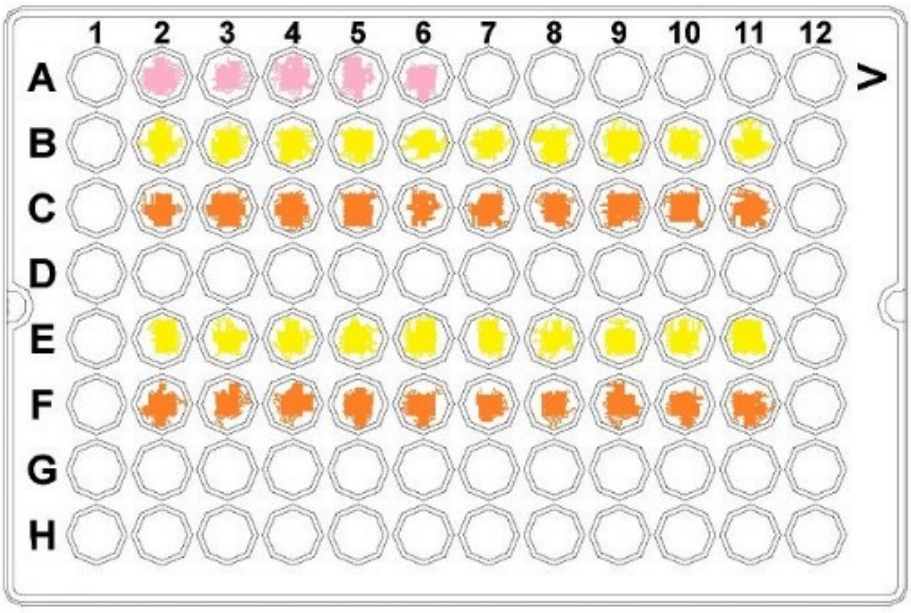

Figure 8| Pipetting scheme for cell viability assay Row A 2 - 6 contained the growth medium (RPMI-1640 or DMEM) only; Row B and E 2 – 11 represented the control, untreated cells; The cells seeded to row C and F 2 – 11 were treated with 20 ng ml^{-1} activin A.

3.5 Enzyme-linked immunosorbent assay (ELISA)

Prior to the ELISA experiment, cells in a sub-confluent state were washed twice with PBS and collected in 500 – 1000 uL RIPA Lysis buffer mixed with HALT protease inhibitor. Cell lysates were than aliquoted in vials and stored at -80°C.

For the assessment of the secreted ActA, logarithmically growing cells in 75 cm^2 cell culture flasks were washed gently twice with PBS and the medium was changed to serum and antibiotic free growth medium. After 24 hours the supernatant of the cell was collected and stored at -20°C.

Human/Mouse/Rat Activin A Quantikine® ELISA kit (R&D Systems, USA) was used to detect patients' plasma ActA levels as well as the secreted and intracellular ActA protein amount in the NSCLC cell lines. Prior to the analysis, samples were defrosted at room temperature. Prior to the measurement 150 μL of plasma was diluted with 150 μL of Calibrator Diluent RD5-54.

200 µL ActA biotinylated antibody was pipetted into each well of the microplate and incubated for 15 minutes at room temperature (RT) on a horizontal orbital microplate shaker set for 500 rpm. Each well was then aspirated and washed with Wash Buffer repeatedly, 3 times.

100 µL of Assay Diluent RD1-98 and 100 µL of standard control or sample was pipetted into each well. The well was then covered and incubated for 3 hours at RT on a horizontal orbital microplate shaker at 500 rpm. Each well was then aspirated and washed with Wash Buffer for total of 5 times.

200 µL ActA Conjugate was added to each well and incubated on the shaker for 1 hour. Washing step was repeated as described above.

200 µL Substrate Solution was added to each well and incubated in the bench drawer (protected from light) for 30 minutes at RT. Lastly, 50 µL Stop Solution was added to each well.

Within 30 minutes the optical density (OD) of the samples were determined using Varioscan Flash microplate reader at 450 nm. Optical imperfections of the plate were corrected using 570 nm values which were subtracted from the readings at 450 nm. The initially established standard curve was used to determine the protein concentrations of the samples.

3.6 SDS-PAGE and Western blot

Cells were seeded into a 6-well plate at a density of 5 x 10^5 cell per well. After 24 hours the cells were washed twice with PBS followed by rh ActA (20 ng ml^{-1}) and mock treatment for 30 min. Cells were harvested in RIPA buffer including Protease inhibitor cocktail and stored at -80°C.

Protein quantification step was performed with the BCA Protein Assay Kit (Thermo Fisher Scientific, USA) with which the required amount of protein lysate for the SDS - polyacrylamide gel electrophoresis (SDS-PAGE) was calculated. The samples were denatured in heat block at 95°C using 5x SLAB solution and cooled down at RT prior to SDS-PAGE.

Mini-PROTEAN™ Tetra electrophoresis chamber, plates and combs (BIORAD, USA) were cleaned with 70% Ethanol and assembled after the acrylamide gels polymerized. Electrophoresis gels were prepared as indicated in **Table 11**. The chamber was filled with pre-cooled running buffer prior to

sample loading. In the first position the ladder was always loaded, followed by the samples' solutions, so that each well equally contains 10 μg protein. After SDS-PAGE the Semi-dry Blotting protocol was followed using BIORAD Blotting Chamber and Amersham™ Protan™ 0,2 μm Nitrocellulose Membrane (GE Healthcare, USA). Immediately after the transfer, the membranes were shortly washed with TBST.

To prevent nonspecific binding of the antibodies the membranes were blocked with 5% non-fat dry milk (NFDM) (BIORAD, USA) for 1 hours at RT. The primary antibody was diluted in 5% NFDM (specific data listed in **Table 12**), added to the Western Blot membranes and incubated overnight. The next day the membranes were washed 5 times in TBST while the secondary antibody solution was prepared in 2,5 % NFDM and subsequently added to the membranes. After one hour incubation the nitrocellulose membranes were washed again 5 times in TBST.

The substrate reagent (Super Signal™, West Femto Maximum Sensitivity Substrate; Thermo Fisher Scientifc, USA) for detection was mixed (500 μL Reagent A and 500 μL Reagent B), pipetted on the membranes and incubated for 5 min while protected from light.

The procedure ends in the dark room (only red light) where the membranes were placed in a film cassette ensuring every air bubble and dirt has been removed. A sheet of Amersham Hyperfilm ECL (GE Healthcare, USA) was taken out of the box and placed on the immobilized membrane. After the exposure the film was developed in the developer machine. The exposure time was increased or decreased depending on the strength of the signal or if the background was high.

Table 11| Recipe for 6 SDS-PAGE gels

Separating gel (10%)	Volumes	**Stacking gel (4%)**	Volumes
Aqua H_2O (B|Braun; Melsungen, Germany)	12,25 mL	Aqua H_2O (B|Braun; Melsungen, Germany)	6,42 mL
4x Running gel buffer pH 8,8	6,25 mL	4x Stacking gel buffer pH 6,8	2,5 mL
40% Acrylamide (GERBU, Heidlberg, Germany)	6,25 mL	40% Acrylamide (GERBU, Heidlberg, Germany)	1 mL
10% SDS	0,25 mL	10% SDS	0,1 mL
10% APS (SIGMA,USA)	100 μL	10% APS (SIGMA, USA)	50 μL
Temed (SIGMA, USA)	25 μL	Temed (SIGMA, USA)	12,5 μL

Table 12| Antibodies used for Western Blot assay

Antibody	Dilution	Supplier	Diluent	Target size (kDa)
Phospho-Smad2 /Smad3 (D27F4) Rabbit mAb	1:500	Cell Signaling	5% NFDM in TBS-T	60/52
Smad2/3 (D7G7) XP® Rabbit mAb	1:1000	Cell Signaling	5% NFDM in TBS-T	60/52
β-Actin (13E5) Rabbit mAb	1:5000	Cell Signaling	5% NFDM in TBS-T	45
Goat anti-Rabbit IgG (H+L) Secondary Antibody, HRP	1:1000	Invitrogen; Thermo Fischer	2,5% NFDM in TBS-T	-

Table 13| List of used solution and buffers during Western blot

Buffer/Solution	Chemical agents	pH
5x Running Buffer	125nM Tris (15 g) 1,25M Glycine (72 g) 0,5% SDS (5 g) 1 L water	8
4x Running gel buffer	36,4 g Tris (1,5 M) 0,8 g SDS 200 mL water	8,8
4x Stacking gel buffer	3,03 g Tris (0,025 M) 0,2 g SDS 50 mL water	6,8
Blotting buffer (Semi dry blotting)	100 mL Trans Blot Turbo 5x Transfer Buffer (BIORAD) 100 mL Absolut Ethanol 300 mL water	
10x Tris-buffered saline (TBS)	24,2 g Tris 80 g NaCl 1 L water	7,6
TBS Tween-20 (TBST)	0,1% Tween-20 in TBS	
10% Sodium dodecyl sulfate (SDS)	5g SDS 50 mL water	
10% Ammoniumpersulfat (APS)	1g APS 10 mL water	
5x SLAB	0,9 g Tris (150 mM) 2,5 g SDS (5%) 12,5 mL glycerol 5,75 mL ß-mercaptoethanol 50 mg bromphenol blue 50 L water	6,8

3.7 *In vivo* Animal experiments

SCID male mice (age: 6 - 8 weeks) obtained from the National Institute of Oncology, Budapest were used in xenograft models, whereas DBA female mice were used to establish syngeneic models. SCID male mice were kept under specific pathogen free (SPF) conditions in National Koranyi Institute of TB and Pulmonology Department of Tumor Biology (Budapest, Hungary). DBA/J2 mice were housed under normal non-pathogen free conditions. Animal experiments were discussed and approved by the "Committee of Animal Protection" of the Hungarian government and conducted according to the Hungarian regulation.

3.7.1 Xenograft model

In xenograft models, immune-deficient animals are inoculated with human tumor derived cells. Model systems are key to identify new drug targets, to evaluate anti-cancer therapies and to screen for novel biomarkers. Mouse is the most used animal for this purpose because of it's cheap maintenance, ease-of-handling and well-studied genetic landscape. [66]

NSCLC cell lines were expanded at "Anna Spiegel Forschungsgebäude" (Austria, Vienna). When the cell count reached 40 million per cell line (calculated via Sysmex XN-350) and the cells were still in the logarithmic growth phase, cells were transferred to the Tumor biology department of the National Koranyi Institute. Upon arrival cells were washed with PBS, trypsinized, harvested in appropriate medium and centrifuged at 149g. Supernatant was discarded and cell pellet was resuspended in serum and antibiotic free RPMI-1640 medium. Viable cell counts were determined using 0,4% trypan blue solution with the cell suspension to obtain 1 to 2 dilution (50 μL of cells and 50 μL of trypan blue). Viable cells (with clear cytoplasm) were counted via hemocytometer. Concentration was adjusted to appropriate densitiy and injected subcutaneously in the right lateral aspect of the thoracic wall according to **Table 14**. Mice were examined every three days where the size of the tumor and the weight of the mice was measured. After the tumor reached 1000 – 1500 mm^3 (calculated as using the formula: $V = (length \times width^2 \times \pi)/6$), the mice were sacrificed by inhalation of isoflurane (Baxter, USA) which was followed by

immediate necropsy. The primary tumors and metastatic lungs were excised and cleaned of any fat tissue, skin and hair. The dissected and cleaned tumor samples and whole lungs were immediately snap-frozen in liquid nitrogen and stored at -80°C.

3.7.2 Syngeneic model

In syngeneic models, mice are injected with tumor cell derived from the same genetic background as the recipient mice. As the syngeneic mice is immunocompetent it is particularly relevant for studies of immune checkpoint inhibitors (CTLA-4, PD-1 inhibitors) [67] or other immunotherapies (CAR-T cells)[68]

KLN-205 squamous cell line was handled as the NSCLC cells except for the initial cell count that was required to perform the experiment outlined in **Table 15**.

Table 14| Mice inoculation plan of NSCLC cells

NSCLC cell line	Xenograft strain	Number of mice injected	Injected cell suspension per mice	Cell density /0,2 mL
VL-1	SCID male	3	0.2 mL	10^7
VL-3	SCID male	3	0.2 mL	10^7
VL-5	SCID male	3	0.2 mL	10^7
VL-7	SCID male	2	0.2 mL	10^7
VL-8	SCID male	3	0.2 mL	10^7
VL-9	SCID male	3	0.2 mL	10^7
VL-10	SCID male	3	0.2 mL	10^7
LUTCML-54	SCID male	3	0.2 mL	10^7
SK-MES-01	SCID male	3	0.2 mL	10^7

Table 15| Mice inoculation plan of KLN-205 syngeneic squamous cell carcinoma cell line

SCC cell line	Syngeneic strain	Number of mice injected	Injected cell suspension per mice	Cell density /0,2 mL
KLN-205	DBA/J2 female	3	0.2 mL	$5x10^5$
KLN-205	DBA/J2 female	4	0.2 mL	10^6
KLN-205	DBA/J2 female	3	0.2 mL	$2x10^6$

4 Results

4.1 Assay of tumorigenicity in mice models

It was intended to assess the tumor forming capacity of the above listed NSCLC cell lines. During the whole experiment the mice were closely monitored where injuries, acute weight loss and any pathological conditions, that would potentially impair the experiment, were observed and recorded. The time of tumor outgrowth upon inoculation and tumor progression were also crucial points of the study. Cell lines, producing predictable and exponential tumor growth are most attractive for later in vivo experiments.

4.1.1 KLN – 205 the syngeneic model

The KLN – 205 cell line was reported to be aggressive and also very metastatic in nature. [69] This experiment was intended to evaluate the tumor forming capacity of the KLN - 205 squamous cell carcinoma cell line, using different cell numbers in syngeneic mice model. Palpable tumors were typically observed within 8 days post inoculation. (**Figure 9**) Tumor aggressiveness is clearly demonstrated since none of the tumor-bearing mice lived past 16 days. Unfortunately, 2 DBA/J2 mice died of unknown reasons in the post injection days, one in the $5x10^5$ group and one in the 10^6 group. Necropsy showed no indication of cancer related death nor visible pathological reasons. Although, there is no considerable difference between group A and B, injection of $2x10^6$ cells yielded in a significantly larger tumor mass. The highest dose also spiked tumor growth which resulted in early death (in 1 week upon tumor appearance).

All animals dose-independently formed tumors which renders this cell line 100% tumorigenic.

4.1.3 Cell Line Derived Xenograft (CDX) mouse model

Contrary to the syngeneic model, the recipient of a CDX is an inbred, immunocompromised, usually rodent animal that was born and raised in a sterile environment. The human NSCLC cells were otherwise rejected by the mice' immune system.

The cell lines VL-1, VL-3 and LUTCML-54 were injected subcutaneously in SCID male mice at a cell density of 10^7 cell/0,2 mL serum free Sigma's RPMI-1640. 5 days following injection, nodules were already palpable at the injection site. After 10 days the previously observed tumors were calipered regularly till the mice' death or till the tumor size reached the maximum when mice were euthanized. The animals were also examined for any clinical sign (wounds, injury, behavioral disorders) and body mass (not shown). All 3 inoculated cell line developed tumors at the injection sites (**Figure 10 A,B,E**) and also formed macroscopic metastases in the lungs but no other macroscopic alteration was detected in other organs or tissues. During the observational phase the tumor volumes' ranged from 708 mm^3 (VL-3; **Figure 10 B**) to 1812 mm^3 (LUTCML-54; **Figure 10 E**). The short latency period and the gradually increasing tumor volume validates these cell lines' malignant potential and therefore suitable as good experimental system for in vivo CDX model.

In contrast, SK-MES-01 and VL-5 (**Figure 10 C,D**) showed weaker experimental value. The latency period in case of VL-5 was 31 days and in case of SK-MES-01 it was 52 days. However, only one mouse developed measurable tumors in each group, with a final volume of approximately 1300 mm^3. The growth rate, however, was more robust in VL-5 that reached it's peak capacity in 2 weeks as opposed to SK-MES-01 which needed 46 days post injection. Regarding their CDX tumor forming potential these cell lines are not suggested for further in vivo experiments. To improve the tumorigenicity, cell lines with lower passage number should be injected in NOD/SCID mice which has not only impaired adaptive immunity but also missing Natural Killer (NK) cells that are in fact very important factors to kill malignant cells that downregulate major histocompatibility complex (MHC) class I molecules [70].

Figure 9| KLN - 205 syngeneic squamous cell carcinoma tumorigenicity assay **A.** 3 DBA/J2 mice were injected with $5x10^5$ cells per mice. **B.** 4 DBA/J2 mice were injected with 10^6 cells per mice **C.** 3 DBA/J2 mice were injected with $2x10^6$ cells per mice

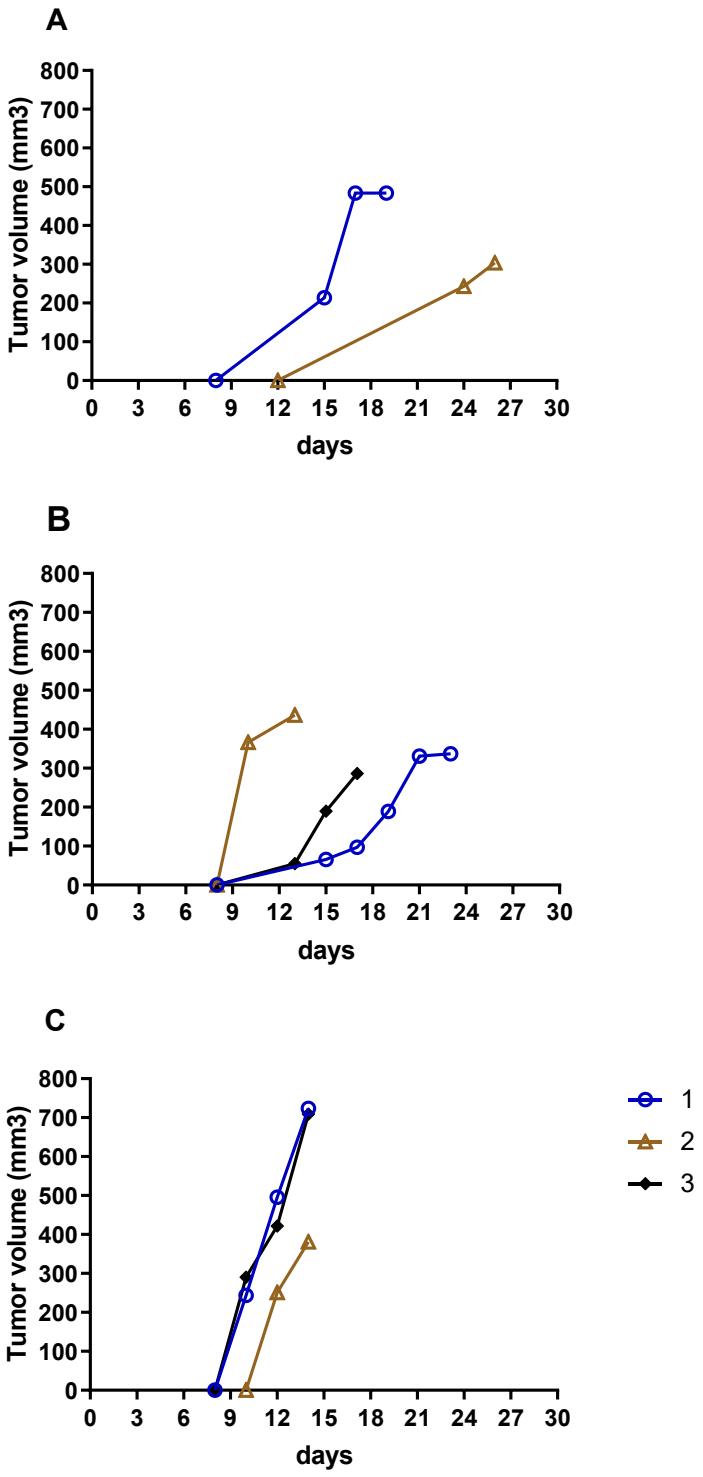

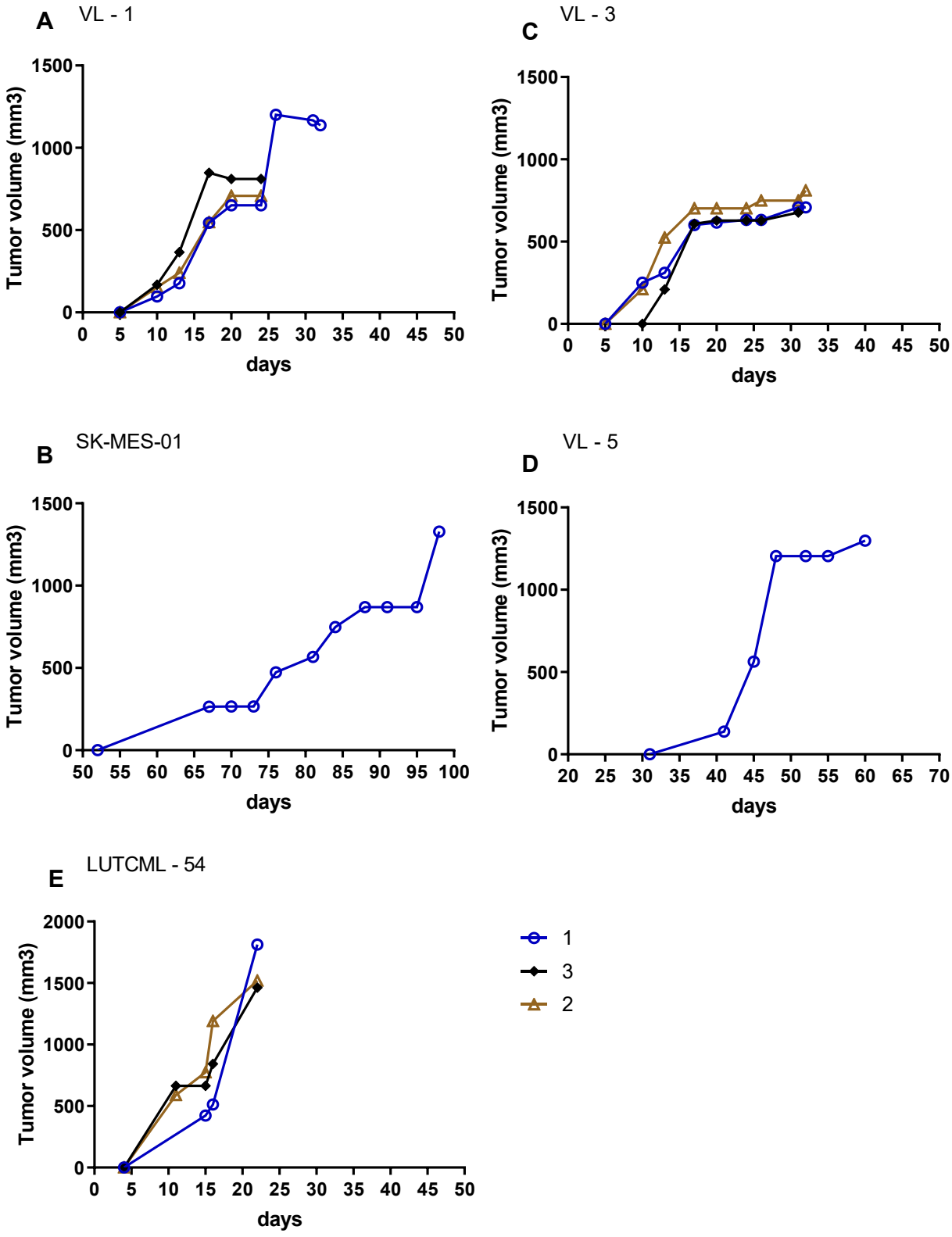
A
VL - 1
Tumor volume (mm3)
days
C
VL - 3
Tumor volume (mm3)
days
B
SK-MES-01
Tumor volume (mm3)
days
D
VL - 5
Tumor volume (mm3)
days
E
LUTCML - 54
Tumor volume (mm3)
days
1
3
2

Figure 10| NSCLC xenograft tumorigenicity assay **A., B., C., D., E.,** 10^7 cells in 200 µL RPMI-1640 was injected subcutaneously in 3 SCID male mice, respectively. Tumor size (width, length) was measured regularly from the outside via a digital caliper.

4.1 RT-qPCR assay for analysis of expression of activin family genes in NSCLC cell lines

To verify that ActA is overexpressed in NSCLC cell lines, I investigated the expression levels of the subunits of ActA (INHBA) as well as the Type I receptor ALK-4 (ActRIB) and the two Type 2 receptor ActRIIA and ActRIIB. The relative expression levels were determined by RT-qPCR using TaqMan assays where GAPDH served as a reference gene.

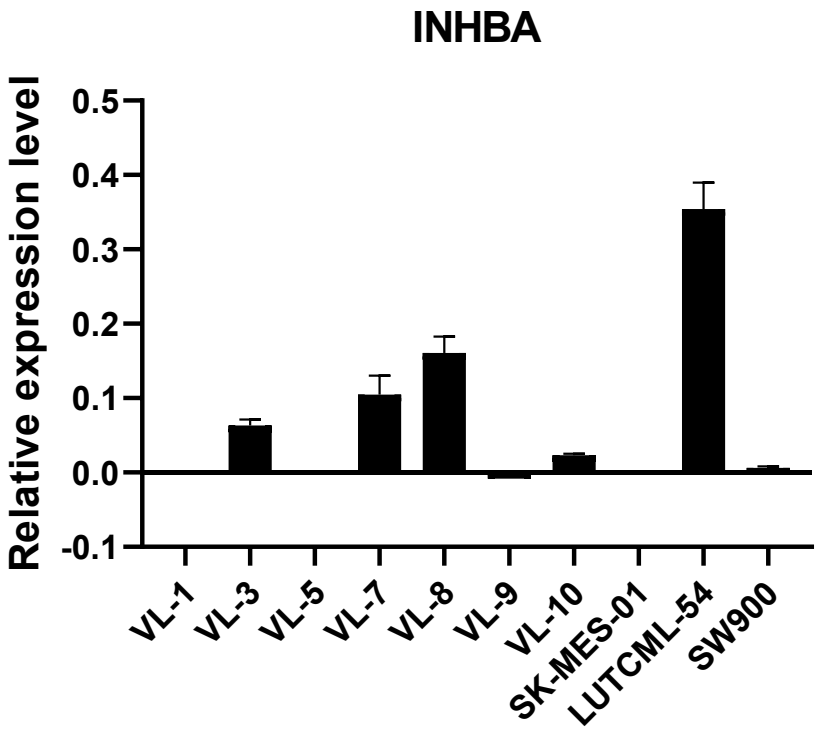

Figure 11| Expression levels of activin subunit ßA (INHBA) in NSCLC cell lines All detectable C_t values were normalized to glyceraldehyde-3 phosphate dehydrogenase (GAPDH) house-keeping gene expression.

Expression of the βA subunit was detected in 5 cell lines (VL-3; VL-7; VL-8; VL-10 and LUTCML-54) and a small amount was also detectable in SW900. (**Figure 11**) The rate of relative expression varies greatly between cell lines considering the 60 fold difference between LUTCML-54 and SW900. The fact that INHBA mRNA is present in half of the cell lines suggest that in lung SCC the patients' elevated ActA levels could be derived from the tumor cells as well.

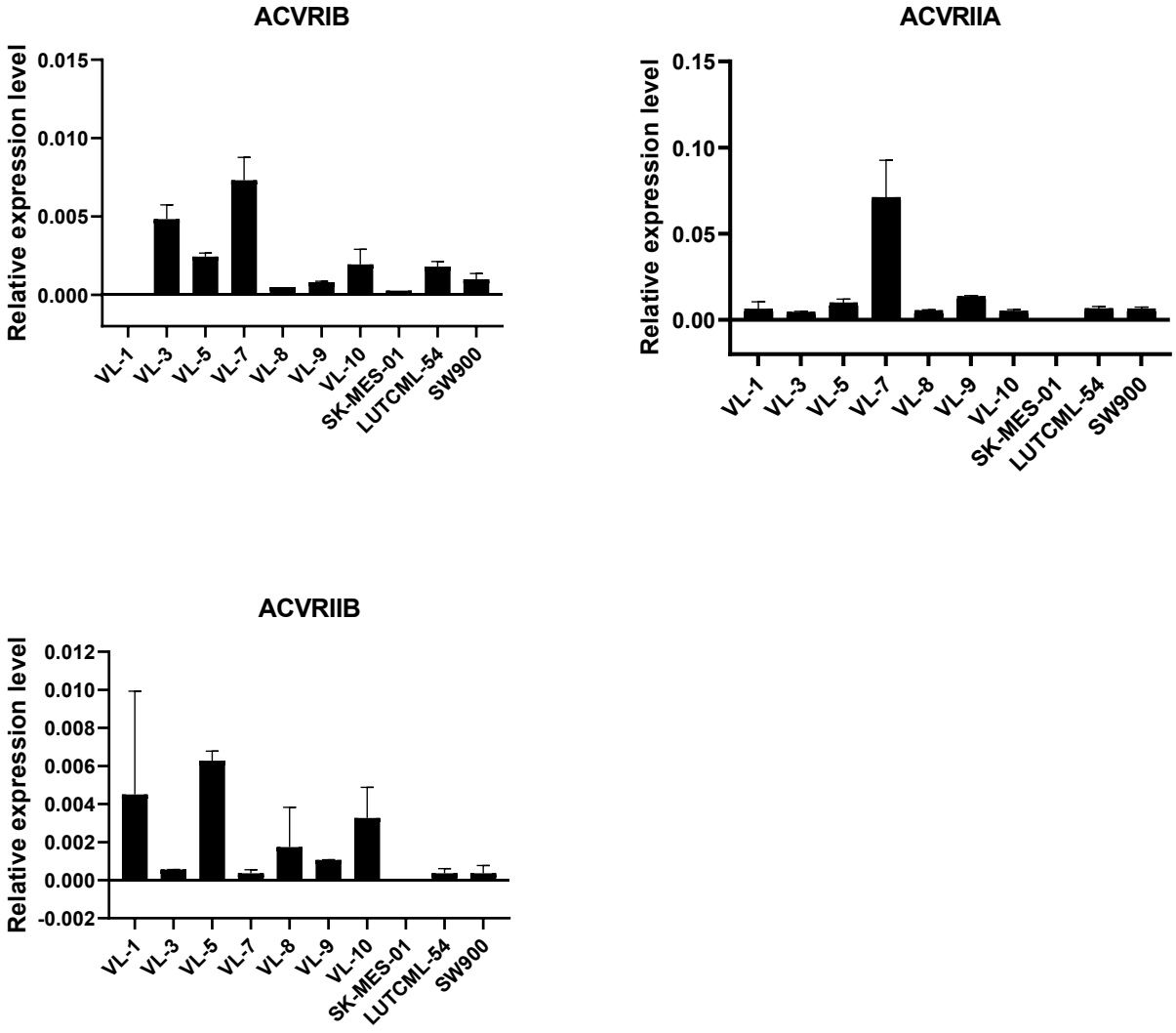

Figure 12| The expression pattern of the Activin A receptors AcvRIB, AcvRIIA and AcvRIIB in NSCLC cell lines All detectable C_t values were normalized to GAPDH house-keeping gene expression.

Upon analysis of the transcript levels of TGF-β family receptors, that are responsible for ActA signaling, it was found that excluding SK-MES-01 all of the cell lines had mRNA transcripts readily present in their cytoplasm(**Figure 12**). In conclusion, those cell lines are presumably able to transduce exogenous recombinant ActA mediated downstream signaling and subsequent receptor mediated Smad2/3 phosphorylation that were both particularly important to identify for later experiments.

4.2 Detection of intracellular and secreted Activin A levels in NSCLC cell lines via ELISA

Human/Mouse/Rat Activin A Quantikine® ELISA kit was used to quantify not only the humans' but also the mice' cell line's (KLN-205) generated ActA protein. According to the manufacturer this ELISA did not show any significant-cross reactivity with other isoforms of ActA or other TGF-β member.

Before the the Smad2/3 phosphorylation assay, the secreted ActA levels had to be measured to establish an initial hypothesis which cell lines will already have a strong active downstream signaling based on the elevated ActA protein levels in the cells' supernatants. However, it is not known whether the antibody used to detect the βA subunit will also detect the FST bound form or exclusively the free ActA. FST was not analyzed in this project, although it's function is to irreversibly bind ActA and abrogate receptor association as well as it facilitates the lysosomal degradation of the Activin A - Follistatin complex.

In line with the qPCR results, the cell lines that displayed detectable INHBA transcripts also presented intra, - and extracellular ActA isoform. In VL-1, VL-5, VL-9 and SK-MES-01 ActA protein was absent as expected from the qPCR values. The RT-qPCR kit was not able to detect mouse ActA transcript therefore in case of KLN-205 only ELISA results are available. The detection limit for the assay was 3000 pg/mL ActA and this amount was proved to be the limitation of the measurement. VL-3 and VL-10 had more secreted whereas LUTCML-54 had more both intra, - and extracellular ActA than the detection limit, therefore these samples have to be diluted before the next assay to have a more precise data on hand (**Figure 13**).

The detected ActA concentrations of the cell's collected supernatants ranged from 75 – 3000 pg/mL, where the lowest and highest were SW900 and LUTCML-54, respectively.

The intracellularly stored ActA amounts did not show significant correlation with the secreted form of our protein of interest. In line with the previous statement, VL-3, VL-10 and KLN-205 cell lines had significantly more stored ActA than secreted. Activin A is tightly regulated at all levels from transcription to receptor binding therefore without assessing the regulatory factors, that are managing the fate of the ActA mRNA till it's mature secreted form eventually binds to a type II receptor, it is quite challenging to derive any conclusion other than that ActA protein is present in SCC cell lines and also readily secreted without exogenous stimulus.

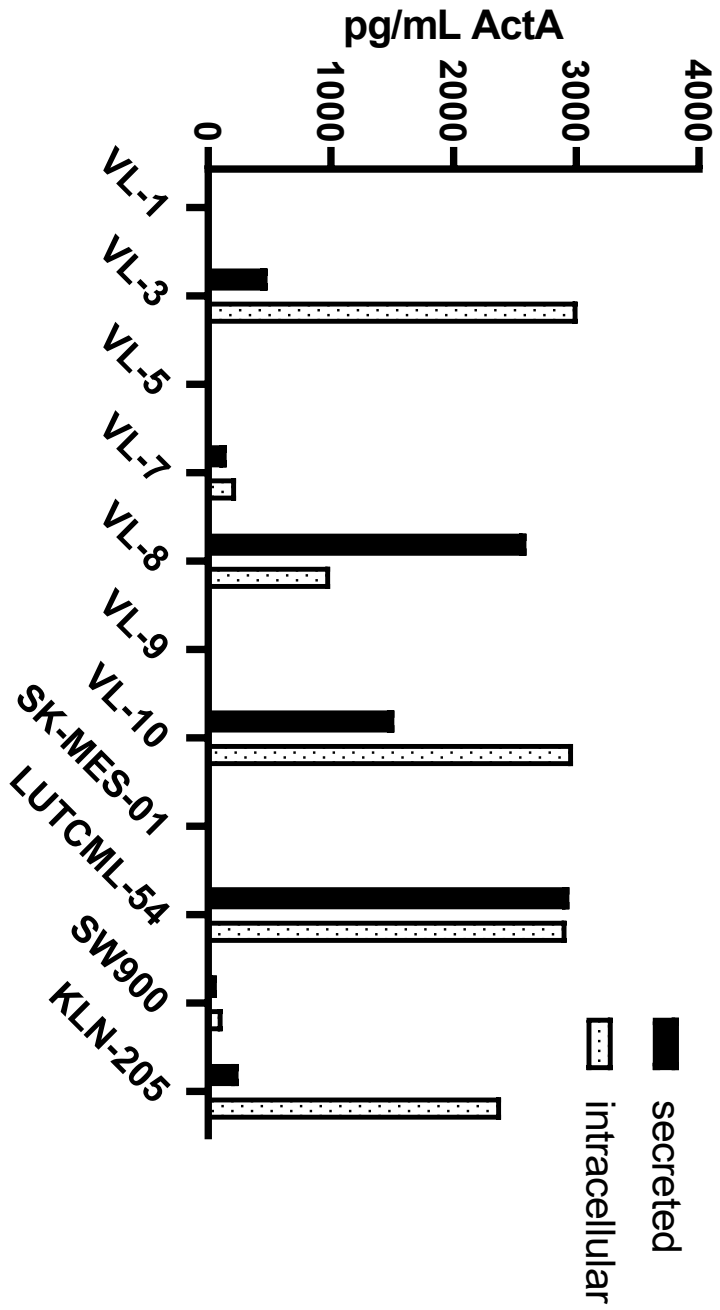

Figure 13*| *Secreted and Intracellular ActA expression confirmed by ELISA measurement 11 NSCLC cell lines' intracellular and secreted ActA levels was measured using Human/Mouse/Rat Activin A Quantikine® ELISA kit

4.3 Cell viability assay using human recombinant Activin A treatment on NSCLC cell lines

We know from our group's previous study that exogenous ActA facilitated the in vitro growth of malignant pleural mesothelioma cells. [71] In contrast, there are studies showing that ActA suppresses breast cancer cell and melanoma cell growth. [60, 72] In order to determine the effect of additional ActA on NSCLC cell proliferation, a cell viability assay was conducted using EZ4U kit. (**Figure 14**)

The result clearly indicates that cell lines expressing activin receptors reacted to recombinant ActA treatment. The TP53 mutant SK-MES-01 SCC cell line, which did not express either the βA subunit of ActA or any receptor transcripts, was not affected by the recombinant ActA. LUTCML-54 was also a non-responder which might be attributed to it's already substantial secreted ActA detected in the cells' supernatant. Additionally, the elevated ActA expression was might coupled with high FST expression as well, hence the reduced bioactivity of hr ActA. Interestingly, the results revealed that following hr ActA treatment for 72 hours, VL-3 and VL-5 SCC cells viability was decreased compared to untreated controls, suggesting that these SCC cell lines did not gain resistance to ActA mediated growth control. As it was rather expected, most of the cell lines benefited from exogenous recombinant ActA treatment, hence the elevated cell proliferation observed in human NSCLC cell lines: VL-1, VL-7, VL-8, VL-9, VL-10 and in squamous mouse cell line: KLN-205. The displayed growth stimulating effect ranged from 7 – 25% compared to mock-treated controls in a 72 hours period. In conclusion, the additional recombinant ActA in the culture media exhibited differential responses in NSCLC cell lines depending on their ability to channel activin signaling.

It has been already determined that NSCLC cell lines express, translate and also secrete ActA. The remaining open question is whether they activate Smad mediated signaling or the effect of ActA treatment was attributed to non-Smad mediated signaling pathways.

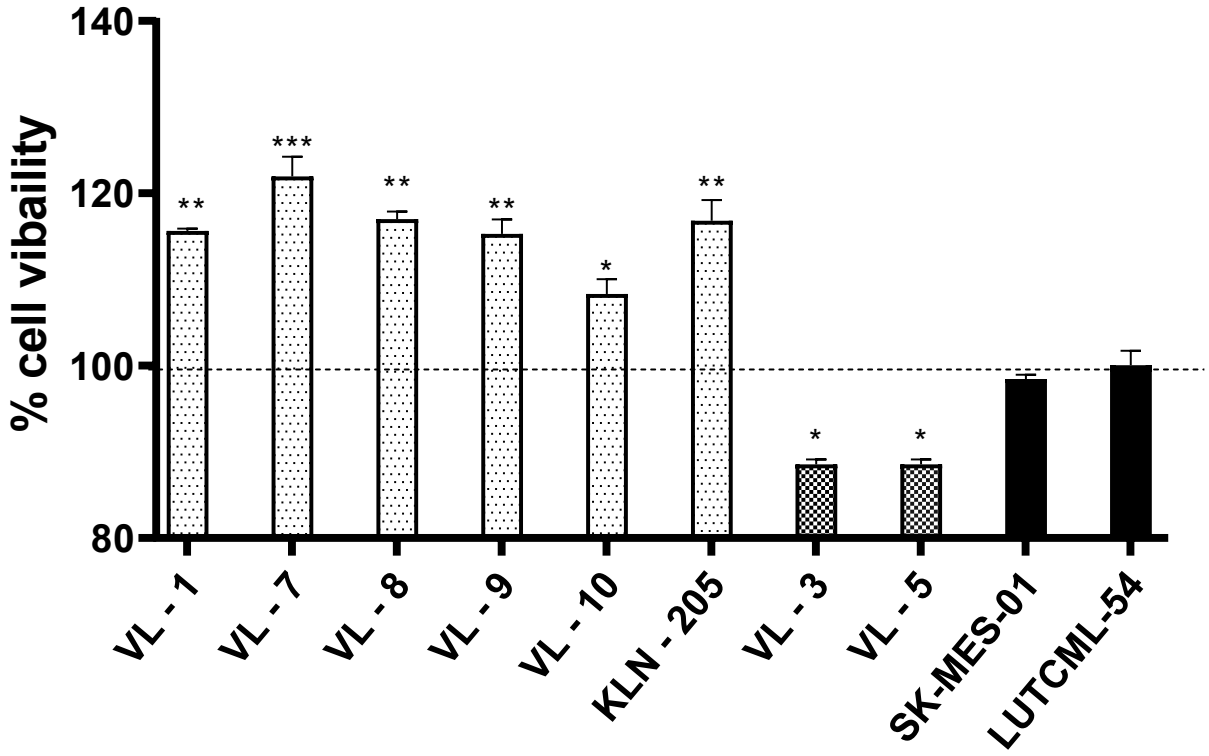

Figure 14| EZ4U cell viability assay on human recombinant Activin A treated NSCLC cell lines *Cell were seeded to 96-well plates according to* Table 10*.*

4.4 Activation of the Smad-mediated signaling via recombinant Activin A treatment

The aim of this assay was to test the induction of SMAD signaling in NSCLC cell lines. To do so cells were seeded to 6-well plates at a density of $5x10^5$ cell per well. After 24 h, cells were washed with PBS and the medium was changed to either 20 ng ml^{-1} ActA containing growth medium or empty growth medium as control. Cells were then incubated for 30 min before collected in RIPA lysis buffer. The used Rabbit mAb detected both P-Smad2 (Ser465/467) and P-Smad3 (Ser423/425) visible in the membrane at 60 kDa and 52 kDa, respectively.

As hypothesized, Smad2 protein was present in all cell lines, however Smad3 expression was not visible in VL-1, VL-5 and VL-7 via this Western Blot.

All of the cell lines displayed detectable difference in Smad phosphorylation compared to mock-treated controls. (**Figure 15**) Although, most of the cell lines showed a considerable Smad phosphorylation even in the control group. In line with our expectations, cell lines that secreted ActA in the supernatant already exerted active downstream signaling prior to ActA treatment. However, VL-3 and VL-9 had no detectable P-Smad prior to ActA treatment of which VL-9 did not present ActA at any measured level. (**Figure 11**; **Figure 13**)

The SCC cell line SK-MES-01 also showed an increased Smad phosphorylation upon activin treatment, despite the fact that there was virtually no ActA receptor present on the mRNA level. (**Figure 12**) The presence of the receptors must be evaluated at the post-translational level.

We hence postulated that recombinant ActA indeed promotes the phosphorylation of Smad2/3 by the initiated receptor-ligand hexameric complex.

It is important to note that Smad2/3 phosphorylation could be attributed to other TGF-β family cytokines, like the TGF-β itself when binds to it's type II receptor and initiates the assembly of the receptor ligand complex activating the Serine/Threonine kinase activity of the type I receptors which subsequently phosphorylates Smad2/3 transcription factors. This conserved canoninal-signaling was described with activins in **Figure 2**.

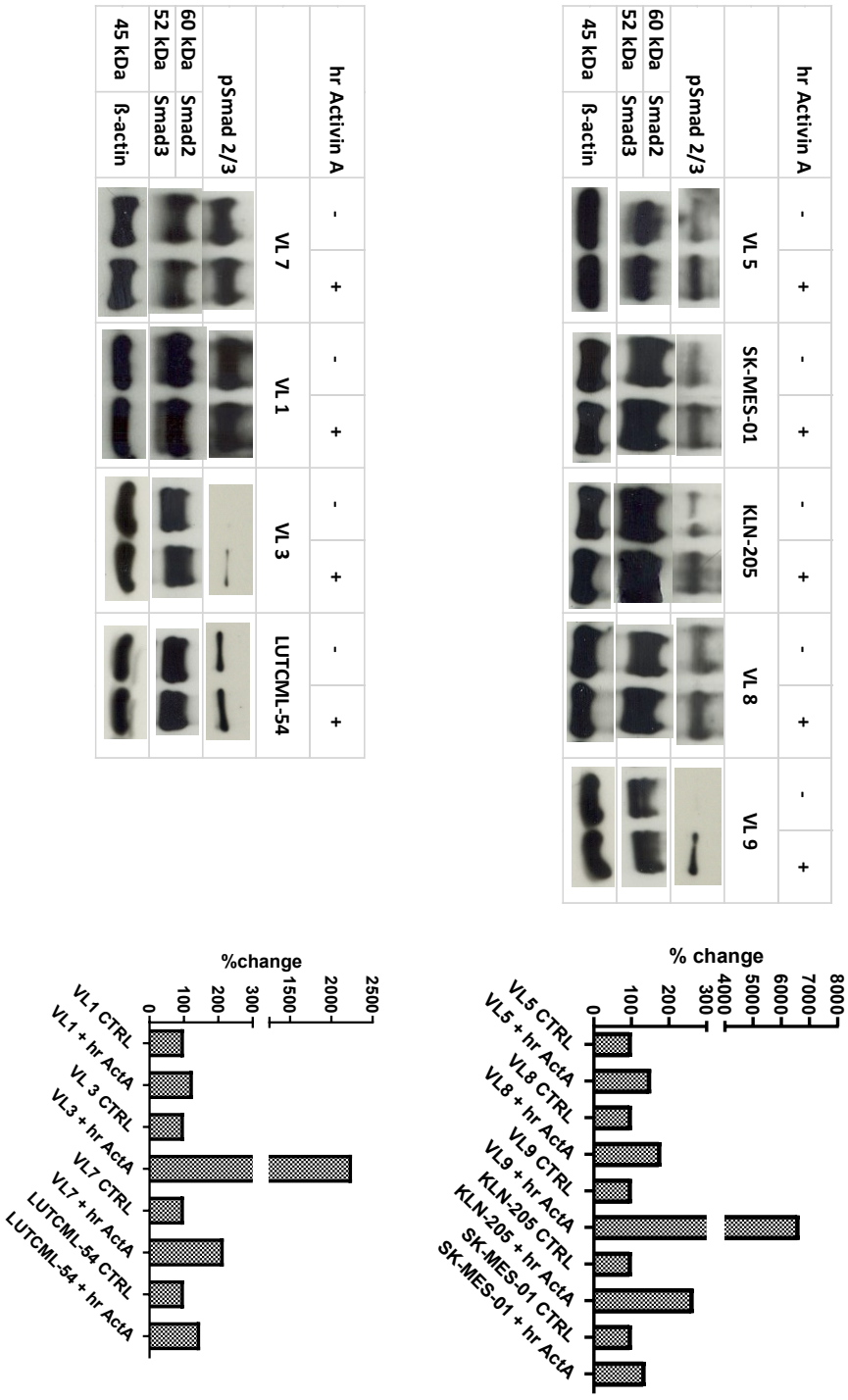

Figure 15| Stimulation of Smad phosphorylation with recombinant ActA containing growth medium in NSCLC cells 20 ng ml^{-1} concentration of human recombinant ActA (hr ActA) was used to treat the cells seeded to 6-well plates – 2 treated well 2 control well per cell line

5 Discussion

Despite the recent improvements of cancer therapy regimen in Squamous Cell Lung Cancer patients, the prognosis remains still poor. The pressure to identify novel clinically useful biomarkers and druggable targets is constantly raising.

Activins were presented as a putative new target in advanced lung cancer, however their diversified roles in various cell types, ranging from embryogenesis, stem cell development, maintenance of homeostasis, cell growth and survival to inflammation makes it difficult to target without interfering with prime mechanism at the cellular and molecular level. [48]

The basic idea that ActA might be overexpressed in SCC patients derived from two 2012 and 2016 study from Hoda et. al. where they measured elevated ActA levels in patients' plasma samples who were suffering from MPM and LADC. Together with this finding, they also reported upregulated ActA levels in various LADC and MPM cell lines. Within the confines of my thesis, we sought to investigate the possible origin of the increased circulating ActA as well as the impact of activin treatment by analyzing patient derived SCC cell lines.

In addition to the preliminary data from our group (**Figure 5**) there was a recent ELISA result of ours which further supported the initial hypothesis, namely: ActA was consistently elevated in SCC patients compared to healthy controls. (**Figure 16**) However, we did not find any correlation between ActA levels and TNM stages in our SCC cohort (**Figure 17**) which was suggested in previous studies as well as in our preliminary data. (**Figure 4;Figure 6**) Upon statistical analysis we did not find any correlation between ActA plasma levels and the patients smoking habits, Body mass index (BMI), COPD status, hypertension and the applied treatment regimen. Nevertheless, ActA is a valid novel biomarker that can help to discriminate lung SCC patients from healthy individuals.

No previous reports have been published regarding the role and the function of ActA in lung SCC, although elevated ActA has been reported in various cancer related studies e.g. lung cancer [54],

esophageal adenocarcinoma [59], oral squamous cell carcinoma [73], gastric cancer [74], therefore it seems that it is a rather general observation. In the above listed thoracic

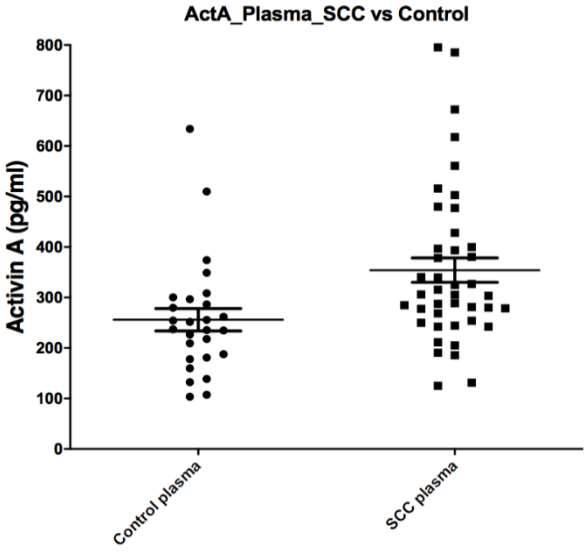

Figure 16|Significantly higher levels of ActA was detected in SCC patients via our latest ELISA n=42; P=0,0014 vs controls (Contribution from: Nicola Uncanin, 2019, Thesis dissertation Bibl. Reference: 3473722)

malignancies it has been stated that ActA's tumor promoting roles overcome the tumor suppressing effect which is in line with my cell viability assay outcome where 6 NSCLC cell lines showed increased proliferation compared to mock-treated control and only 2 of the cell lines reported negative effects upon recombinant ActA treatment. (**Figure 14**) The growth inhibitory effect of ActA in cancer cells can be evaded by various mechanisms: inactivating mutation in type I and type II receptors [55, 75] upregulation the activin antagonist FST [76], Smad4 Loss of Heterozygosity [62] [77, 78] and amplification of non-Smad antagonists Smurf1/2 [79]. In our SCC cell lines, however, the canonical activin signaling has proven to be intact due to the induction of Smad2 phosphorylation upon recombinant ActA treatment and also the validated presence of the activin receptors. Therefore, assessment of FST levels in SCC cell lines is highly desirable which would provide better understanding of the regulatory mechanism in activin signaling.

The formation and the subsequent nuclear translocation of the Smad/2/3/4 complex has a strong cell cycle regulatory effect by controlling the expression of $p15^{INK4B}$**,** $p21^{WAF1/Cip1}$, $p16^{INK4A}$, cyclin A, cyclin D1 and cyclin E [53**,** 80**,** 81]. The cyclin dependent kinase inhibitor (CDKI) $p15^{INK4B}$ induce apoptosis and cell cycle arrest which is considered to be the main activity of the activin signaling.

[82] In addition, overexpression of FST can mitigate ActA's tumor-promoting nature in many ways. Primarily, it can abolish the association of ActA with the type II receptor hence decreasing the concentration of bioavailable ActA. [83] Thus, it explains the ActA induced proliferation arrest in VL-3 and VL-5 cell lines.

Conversely, the growth stimulatory effects of ActA in lung cancer cases are not well documented. Several studies attributed ActA's tumor promoting effect to signaling through non-canonical pathways. [84] [83, 85] For instance, PI3K pathway has been shown to mitigate TGF-β-induced apoptosis and cell cycle arrest in various tumour cell lines.[86-88] Moreover, a recent finding demonstrated a novel role for PI3K when together with mTORC2 they facilitate Smad2/3 proteosomal degradation via Nedd4L E3- Ubiquitin-Ligase[89]. In addition, canonical Wnt/β-catenin signaling that is one well studied oncogenic pathway found deregulated in various cancers. [90] There is a growing body of evidence that cross-talk between the TGF-β and Wnt/β-catenin pathway is key in induction of epithelial mesenchymal transition (EMT) which is one of the main drivers of metastasis formation. [91] Activins have been reported to activate p38MAPK/ERK1/2 pathway in a Smad-independent fashion, which was linked to promotion of angiogenesis and migration. [92] [93] These promising findings have yet to be confirmed in squamous cell lung cancer cells.

Activins exert their biological effect by binding to their receptors, which when activated phosphorylate the Smad proteins. TGF-β, activin and nodal, members of the TGF-β superfamily, all use Smad2 and Smad3 to facilitate the transcription of their target genes. [94] To elucidate whether ActA can activate the Serine/Threonine kinase activity of the type I and type II receptors and in turn phosphorylate Smad2/3, cells were seeded to 6-well plates at a density of $5x10^5$ and treated with 20 ng ml^{-1} hr ActA or mock. Treated cells showed consistent Smad2 phosphorylation even though most of the cell lines had already visible P-Smad2 signal in the control group. Those cell lines had active downstream signaling possibly because of the presence of TGF-β, activins or nodal. Despite VL-1 LADC cell line had no detectable ActA on any levels it had an enhanced P-Smad2 band at 60 kDa therefore it is obvious that not only ActA can activate the receptor mediated phosphorylation of the Smad2/3 complex.

To lay down the foundation of later *in vivo* experiments we performed a series of tumorigenicity assays to assess the tumor forming capacity of our NSCLC cell lines. Subcutaneously injected immunocompromised mouse models are frequently used to evaluate anti-tumor activities of novel drugs or combination treatments. These models are also eligible to study the pathogenesis of certain tumors transfected with specifically constructed lentiviral vectors that are stably expressing our protein of interest. Lentiviral vectors expressing ActA or it's best studied antagonist FST are promising future candidates for our CDX models. The chosen cell line is highly dependent on the experiment per se because every subtype has a different prognosis and treatment response hence leading us to the wrong conclusion.

Here we demonstrate that ActA is in fact expressed by 7 of 11 SCC cell lines, evidenced by the detected βA subunit of ActA which observation was later validated with ELISA where intracellular and secreted ActA protein was quantified. We did not find any correlation between high ActA expression and *in vivo* tumor forming capacity. On the other hand, we found that recombinant ActA treatment influenced NSCLC cell growth, although there was no clear connection between ActA expression and how the cells reacted to the treatment. Hr ActA inhibited cellular proliferation in VL-3 and VL-5 cell lines via the canonical Smad-signaling and supported VL-1, VL-7, VL-8, VL-9, VL-10 and KLN-205 cell lines' growth using supposedly non-canonical pathways. Finally, to confirm the intact activin-Smad signaling cascade, first we determined the presence of ActA receptor transcripts followed by ActA induced Smad2/3 phosphorylation test. To gain better understanding in the regulatory and growth stimulatory effects of ActA further *in vitro* experiments has to be conducted in the future.

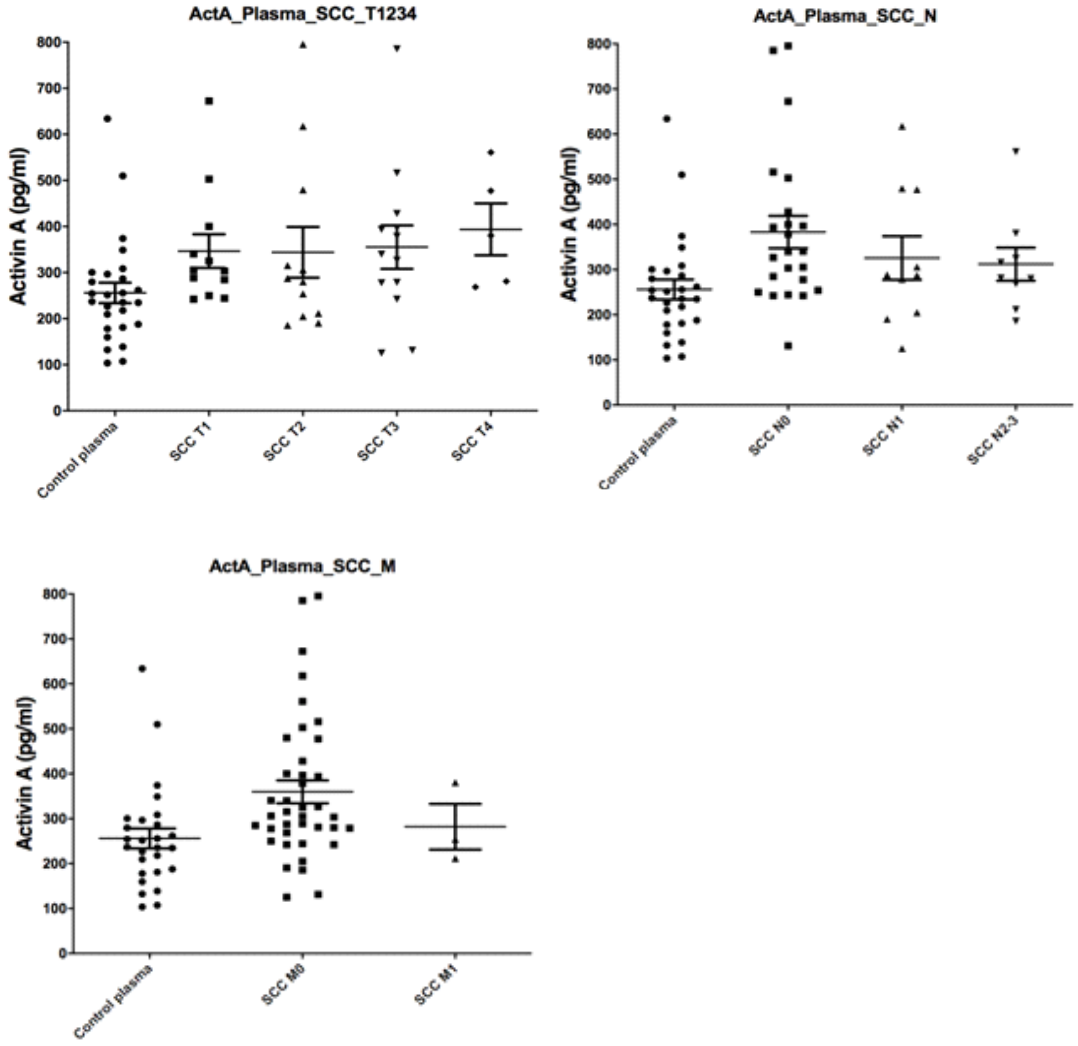

Figure 17| ActA plasma levels in controls and SCC patients in respect to their TNM status
(Contribution from: Nicola Uncanin, 2019, Thesis dissertation Bibl. Reference: 3473722)

6 References

1. Torre, L.A., et al., *Global cancer statistics, 2012.* CA Cancer J Clin, 2015. **65**(2): p. 87-108.
2. Molina, J.R., et al., *Non-Small Cell Lung Cancer: Epidemiology, Risk Factors, Treatment, and Survivorship.* Mayo Clinic Proceedings, 2008. **83**(5): p. 584-594.
3. Detterbeck, F. and L. Molins, *Video-assisted thoracic surgery and open chest surgery in lung cancer treatment: present and future.* Journal of visualized surgery, 2016. **2**: p. 173-173.
4. Tarsitano, A., M.L. Tardio, and C. Marchetti, *Impact of perineural invasion as independent prognostic factor for local and regional failure in oral squamous cell carcinoma.* Oral Surgery, Oral Medicine, Oral Pathology and Oral Radiology, 2015. **119**(2): p. 221-228.
5. Youlden, D.R., S.M. Cramb, and P.D. Baade, *The International Epidemiology of Lung Cancer: geographical distribution and secular trends.* J Thorac Oncol, 2008. **3**(8): p. 819-31.
6. Travis, W.D., et al., *The 2015 World Health Organization Classification of Lung Tumors: Impact of Genetic, Clinical and Radiologic Advances Since the 2004 Classification.* J Thorac Oncol, 2015. **10**(9): p. 1243-1260.
7. Alberg, A.J., M.V. Brock, and J.M. Samet, *Epidemiology of lung cancer: looking to the future.* J Clin Oncol, 2005. **23**(14): p. 3175-85.
8. Papi, A., et al., *COPD increases the risk of squamous histological subtype in smokers who develop non-small cell lung carcinoma.* Thorax, 2004. **59**(8): p. 679-681.
9. Bozinovski, S., et al., *COPD and squamous cell lung cancer: aberrant inflammation and immunity is the common link.* Br J Pharmacol, 2016. **173**(4): p. 635-48.
10. *Comprehensive genomic characterization of squamous cell lung cancers.* Nature, 2012. **489**(7417): p. 519-25.
11. Herbst, R.S., D. Morgensztern, and C. Boshoff, *The biology and management of non-small cell lung cancer.* Nature, 2018. **553**: p. 446.
12. Zhang, X.-C., et al., *Comprehensive genomic and immunological characterization of Chinese non-small cell lung cancer patients.* Nature communications, 2019. **10**(1): p. 1772-1772.
13. Brahmer, J., et al., *Nivolumab versus Docetaxel in Advanced Squamous-Cell Non-Small-Cell Lung Cancer.* N Engl J Med, 2015. **373**(2): p. 123-35.
14. Zhang, H., et al., *Lobaplatin for the treatment of SK-MES-1 lung squamous cell line in vitro and in vivo.* Onco Targets Ther, 2016. **9**: p. 4215-24.
15. Linden, D., K. Linden, and J. Oparka, *In patients with resectable non-small-cell lung cancer, is video-assisted thoracoscopic segmentectomy a suitable alternative to thoracotomy and segmentectomy in terms of morbidity and equivalence of resection?* Interact Cardiovasc Thorac Surg, 2014. **19**(1): p. 107-10.
16. British Thoracic, S., B. Society of Cardiothoracic Surgeons of Great, and P. Ireland Working, *BTS guidelines: guidelines on the selection of patients with lung cancer for surgery.* Thorax, 2001. **56**(2): p. 89-108.
17. Filosso, P.L., et al., *Primary lung tumors invading the chest wall.* Journal of thoracic disease, 2016. **8**(Suppl 11): p. S855-S862.
18. Provencio, M., et al., *Inoperable stage III non-small cell lung cancer: Current treatment and role of vinorelbine.* Journal of thoracic disease, 2011. **3**(3): p. 197-204.
19. Mantovani, F., L. Collavin, and G. Del Sal, *Mutant p53 as a guardian of the cancer cell.* Cell Death & Differentiation, 2019. **26**(2): p. 199-212.
20. Nitiss, J.L., *Targeting DNA topoisomerase II in cancer chemotherapy.* Nature reviews. Cancer, 2009. **9**(5): p. 338-350.

21. Sosa Iglesias, V., et al., *Drug Resistance in Non-Small Cell Lung Cancer: A Potential for NOTCH Targeting?* Frontiers in oncology, 2018. **8**: p. 267-267.
22. Winer, A., J.N. Bodor, and H. Borghaei, *Identifying and managing the adverse effects of immune checkpoint blockade.* Journal of thoracic disease, 2018. **10**(Suppl 3): p. S480-S489.
23. Liao, R.G., et al., *Targeted therapy for squamous cell lung cancer.* Lung cancer management, 2012. **1**(4): p. 293-300.
24. Chan, B.A. and B.G.M. Hughes, *Targeted therapy for non-small cell lung cancer: current standards and the promise of the future.* Translational lung cancer research, 2015. **4**(1): p. 36-54.
25. Derman, B.A., et al., *Treatment of advanced squamous cell carcinoma of the lung: a review.* Transl Lung Cancer Res, 2015. **4**(5): p. 524-32.
26. Garon, E.B., et al., *Ramucirumab plus docetaxel versus placebo plus docetaxel for second-line treatment of stage IV non-small-cell lung cancer after disease progression on platinum-based therapy (REVEL): a multicentre, double-blind, randomised phase 3 trial.* The Lancet, 2014. **384**(9944): p. 665-673.
27. Jotte, R.M., et al., *IMpower131: Primary PFS and safety analysis of a randomized phase III study of atezolizumab + carboplatin + paclitaxel or nab-paclitaxel vs carboplatin + nab-paclitaxel as 1L therapy in advanced squamous NSCLC.* Journal of Clinical Oncology, 2018. **36**(18_suppl): p. LBA9000-LBA9000.
28. Salgia, R., et al., *Role of serum tumor markers CA 125 and CEA in non-small cell lung cancer.* Anticancer Res, 2001. **21**(2B): p. 1241-6.
29. Khan, N., et al., *Clinical utility of serum amyloid A and macrophage migration inhibitory factor as serum biomarkers for the detection of nonsmall cell lung carcinoma.* Cancer, 2004. **101**(2): p. 379-84.
30. Kang, S.M., et al., *The Haptoglobin beta chain as a supportive biomarker for human lung cancers.* Mol Biosyst, 2011. **7**(4): p. 1167-75.
31. Cheng, T., et al., *Correlation of apolipoprotein A-I kinetics with survival and response to first-line platinum-based chemotherapy in advanced non-small cell lung cancer.* Med Oncol, 2015. **32**(1): p. 407.
32. Korbakis, D., et al., *Serum LAMC2 enhances the prognostic value of a multi-parametric panel in non-small cell lung cancer.* Br J Cancer, 2015. **113**(3): p. 484-91.
33. Zhu, J.F., et al., *High plasma fibrinogen concentration and platelet count unfavorably impact survival in non-small cell lung cancer patients with brain metastases.* Chin J Cancer, 2014. **33**(2): p. 96-104.
34. Unal, D., et al., *Is Human Kallikrein 11 in Non-small Cell Lung Cancer Treated Chemoradiotherapy Associated with Survival?* Cancer Res Treat, 2016. **48**(1): p. 98-105.
35. Rolfo, C., et al., *Liquid biopsies in lung cancer: The new ambrosia of researchers.* Biochimica et Biophysica Acta (BBA) - Reviews on Cancer, 2014. **1846**(2): p. 539-546.
36. Weber, D.G., et al., *Evaluation of long noncoding RNA MALAT1 as a candidate blood-based biomarker for the diagnosis of non-small cell lung cancer.* BMC Research Notes, 2013. **6**(1): p. 518.
37. Rodgarkia-Dara, C., et al., *The activin axis in liver biology and disease.* Mutat Res, 2006. **613**(2-3): p. 123-37.
38. Ling, N., et al., *A homodimer of the beta-subunits of inhibin A stimulates the secretion of pituitary follicle stimulating hormone.* Biochem Biophys Res Commun, 1986. **138**(3): p. 1129-37.
39. Ling, N., et al., *Pituitary FSH is released by a heterodimer of the beta-subunits from the two forms of inhibin.* Nature, 1986. **321**(6072): p. 779-82.
40. Jones, K.L., et al., *Activin A and follistatin in systemic inflammation.* Mol Cell Endocrinol, 2004. **225**(1-2): p. 119-25.

41. Beattie, G.M., et al., *Activin A maintains pluripotency of human embryonic stem cells in the absence of feeder layers.* Stem Cells, 2005. **23**(4): p. 489-95.
42. Hubner, G., et al., *Strong induction of activin expression after injury suggests an important role of activin in wound repair.* Dev Biol, 1996. **173**(2): p. 490-8.
43. Namwanje, M. and C.W. Brown, *Activins and Inhibins: Roles in Development, Physiology, and Disease.* Cold Spring Harb Perspect Biol, 2016. **8**(7).
44. Ogawa, K., et al., *Activin A functions as a Th2 cytokine in the promotion of the alternative activation of macrophages.* J Immunol, 2006. **177**(10): p. 6787-94.
45. Ebert, S., et al., *Microglial cells and peritoneal macrophages release activin A upon stimulation with Toll-like receptor agonists.* Neuroscience Letters, 2007. **413**(3): p. 241-244.
46. Robson, N.C., et al., *Activin-A: a novel dendritic cell–derived cytokine that potently attenuates CD40 ligand–specific cytokine and chemokine production.* Blood, 2008. **111**(5): p. 2733.
47. Funaba, M., et al., *Role of activin A in murine mast cells: modulation of cell growth, differentiation, and migration.* J Leukoc Biol, 2003. **73**(6): p. 793-801.
48. Tsuchida, K., et al., *Activin signaling as an emerging target for therapeutic interventions.* Cell Commun Signal, 2009. **7**: p. 15.
49. Walton, K.L., et al., *A common biosynthetic pathway governs the dimerization and secretion of inhibin and related transforming growth factor beta (TGFbeta) ligands.* The Journal of biological chemistry, 2009. **284**(14): p. 9311-9320.
50. Zhang, Y.E., *Non-Smad pathways in TGF-beta signaling.* Cell research, 2009. **19**(1): p. 128-139.
51. Kavsak, P., et al., *Smad7 binds to Smurf2 to form an E3 ubiquitin ligase that targets the TGF beta receptor for degradation.* Mol Cell, 2000. **6**(6): p. 1365-75.
52. Jeruss, J.S., et al., *Down-regulation of activin, activin receptors, and Smads in high-grade breast cancer.* Cancer Res, 2003. **63**(13): p. 3783-90.
53. Razanajaona, D., et al., *Silencing of FLRG, an antagonist of activin, inhibits human breast tumor cell growth.* Cancer Res, 2007. **67**(15): p. 7223-9.
54. Seder, C.W., et al., *Upregulated INHBA expression may promote cell proliferation and is associated with poor survival in lung adenocarcinoma.* Neoplasia, 2009. **11**(4): p. 388-96.
55. Hempen, P.M., et al., *Evidence of selection for clones having genetic inactivation of the activin A type II receptor (ACVR2) gene in gastrointestinal cancers.* Cancer Res, 2003. **63**(5): p. 994-9.
56. Kang, H.Y., et al., *Activin A enhances prostate cancer cell migration through activation of androgen receptor and is overexpressed in metastatic prostate cancer.* J Bone Miner Res, 2009. **24**(7): p. 1180-93.
57. Do, T.V., et al., *The role of activin A and Akt/GSK signaling in ovarian tumor biology.* Endocrinology, 2008. **149**(8): p. 3809-16.
58. Grusch, M., et al., *Deregulation of the activin/follistatin system in hepatocarcinogenesis.* J Hepatol, 2006. **45**(5): p. 673-80.
59. Seder, C.W., et al., *INHBA overexpression promotes cell proliferation and may be epigenetically regulated in esophageal adenocarcinoma.* J Thorac Oncol, 2009. **4**(4): p. 455-62.
60. Stove, C., et al., *Melanoma cells secrete follistatin, an antagonist of activin-mediated growth inhibition.* Oncogene, 2004. **23**(31): p. 5330-9.
61. Yoshinaga, K., et al., *Activin a causes cancer cell aggressiveness in esophageal squamous cell carcinoma cells.* Ann Surg Oncol, 2008. **15**(1): p. 96-103.
62. Hoda, M.A., et al., *High circulating activin A level is associated with tumor progression and predicts poor prognosis in lung adenocarcinoma.* Oncotarget, 2016. **7**(12): p. 13388-99.
63. Hoda, M.A., et al., *Circulating activin A is a novel prognostic biomarker in malignant pleural mesothelioma - A multi-institutional study.* Eur J Cancer, 2016. **63**: p. 64-73.

64. Berger, W., et al., *Expression of the multidrug resistance-associated protein (MRP) and chemoresistance of human non-small-cell lung cancer cells.* Int J Cancer, 1997. **73**(1): p. 84-93.
65. Kaneko, T. and G.A. LePage, *Growth characteristics and drug responses of a murine lung carcinoma in vitro and in vivo.* Cancer Res, 1978. **38**(7): p. 2084-90.
66. Jung, J., *Human tumor xenograft models for preclinical assessment of anticancer drug development.* Toxicological research, 2014. **30**(1): p. 1-5.
67. Poon, E., et al., *The MEK inhibitor selumetinib complements CTLA-4 blockade by reprogramming the tumor immune microenvironment.* J Immunother Cancer, 2017. **5**(1): p. 63.
68. Kueberuwa, G., et al., *A Syngeneic Mouse B-Cell Lymphoma Model for Pre-Clinical Evaluation of CD19 CAR T Cells.* J Vis Exp, 2018(140).
69. Kaneko, T. and G.A. LePage, *Growth Characteristics and Drug Responses of a Murine Lung Carcinoma in Vitro and <em>in Vivo</em&gt.* Cancer Research, 1978. **38**(7): p. 2084.
70. Morvan, M.G. and L.L. Lanier, *NK cells and cancer: you can teach innate cells new tricks.* Nature Reviews Cancer, 2015. **16**: p. 7.
71. Hoda, M.A., et al., *Suppression of activin A signals inhibits growth of malignant pleural mesothelioma cells.* British journal of cancer, 2012. **107**(12): p. 1978-1986.
72. Burdette, J.E., et al., *Activin A mediates growth inhibition and cell cycle arrest through Smads in human breast cancer cells.* Cancer Res, 2005. **65**(17): p. 7968-75.
73. Chang, K.P., et al., *Overexpression of activin A in oral squamous cell carcinoma: association with poor prognosis and tumor progression.* Ann Surg Oncol, 2010. **17**(7): p. 1945-56.
74. Wang, Q., et al., *Upregulated INHBA expression is associated with poor survival in gastric cancer.* Med Oncol, 2012. **29**(1): p. 77-83.
75. Su, G.H., et al., *ACVR1B (ALK4, activin receptor type 1B) gene mutations in pancreatic carcinoma.* Proceedings of the National Academy of Sciences of the United States of America, 2001. **98**(6): p. 3254-3257.
76. Rodgarkia, C., et al., *The activin axis in liver biology and disease*. Vol. 613. 2006. 123-37.
77. Levy, L. and C.S. Hill, *Alterations in components of the TGF-beta superfamily signaling pathways in human cancer.* Cytokine Growth Factor Rev, 2006. **17**(1-2): p. 41-58.
78. Hahn, S.A., et al., *Allelotype of pancreatic adenocarcinoma using xenograft enrichment.* Cancer Res, 1995. **55**(20): p. 4670-5.
79. Samanta, D. and P.K. Datta, *Alterations in the Smad pathway in human cancers.* Frontiers in bioscience (Landmark edition), 2012. **17**: p. 1281-1293.
80. Pardali, K., et al., *Smad pathway-specific transcriptional regulation of the cell cycle inhibitor p21(WAF1/Cip1).* J Cell Physiol, 2005. **204**(1): p. 260-72.
81. Chen, Y.-G., et al., *Activin Signaling and Its Role in Regulation of Cell Proliferation, Apoptosis, and Carcinogenesis.* Experimental Biology and Medicine, 2006. **231**(5): p. 534-544.
82. Ho, J., et al., *Activin induces hepatocyte cell growth arrest through induction of the cyclin-dependent kinase inhibitor p15INK4B and Sp1.* Cellular signalling, 2004. **16**(6): p. 693-701.
83. Grusch, M., et al., *The crosstalk of RAS with the TGF-beta family during carcinoma progression and its implications for targeted cancer therapy.* Curr Cancer Drug Targets, 2010. **10**(8): p. 849-57.
84. Bauer, J., et al., *Activin and TGFβ use diverging mitogenic signaling in advanced colon cancer.* Molecular cancer, 2015. **14**: p. 182-182.
85. Dean, M., D.A. Davis, and J.E. Burdette, *Activin A stimulates migration of the fallopian tube epithelium, an origin of high-grade serous ovarian cancer, through non-canonical signaling.* Cancer letters, 2017. **391**: p. 114-124.

86. Chen, R.H., et al., *Suppression of transforming growth factor-beta-induced apoptosis through a phosphatidylinositol 3-kinase/Akt-dependent pathway.* Oncogene, 1998. **17**(15): p. 1959-68.
87. Conery, A.R., et al., *Akt interacts directly with Smad3 to regulate the sensitivity to TGF-beta induced apoptosis.* Nat Cell Biol, 2004. **6**(4): p. 366-72.
88. Remy, I., A. Montmarquette, and S.W. Michnick, *PKB/Akt modulates TGF-beta signalling through a direct interaction with Smad3.* Nat Cell Biol, 2004. **6**(4): p. 358-65.
89. Yu, J.S., et al., *PI3K/mTORC2 regulates TGF-beta/Activin signalling by modulating Smad2/3 activity via linker phosphorylation.* Nat Commun, 2015. **6**: p. 7212.
90. Polakis, P., *The many ways of Wnt in cancer.* Curr Opin Genet Dev, 2007. **17**(1): p. 45-51.
91. Cai, J., et al., *Simultaneous overactivation of Wnt/β-catenin and TGFβ signalling by miR-128-3p confers chemoresistance-associated metastasis in NSCLC.* Nature Communications, 2017. **8**: p. 15870.
92. Wagner, K., et al., *Activin A stimulates vascular endothelial growth factor gene transcription in human hepatocellular carcinoma cells.* Gastroenterology, 2004. **126**(7): p. 1828-43.
93. Zhang, L., et al., *MEKK1 transduces activin signals in keratinocytes to induce actin stress fiber formation and migration.* Mol Cell Biol, 2005. **25**(1): p. 60-5.
94. Ethier, J.F. and J.K. Findlay, *Roles of activin and its signal transduction mechanisms in reproductive tissues.* Reproduction, 2001. **121**(5): p. 667-75.
95. Dr.Med.Thomas Klikovits, *Translational relevance of Activin A in human squamous cell lung cancer: an international two-center study*

7 List of figures

8 List of tables